FLORIDA STATE UNIVERSITY

COLLEGE OF ARTS AND SCIENCES

THE CHARACTERIZATION OF THE VARIABILITY OF THE WET SEASON OVER CENTRAL AMERICA

By

JOANNA RODGERS

A Thesis submitted to the
Department of Earth, Ocean, and Atmospheric Science
in partial fulfillment of the
requirements for the degree of
Master of Meteorology

2023

Joanna Rodgers defended this thesis on November 2, 2023.
The members of the supervisory committee were:

Vasubandhu Misra
Professor Directing Thesis

Robert Hart
Committee Member

Allison Wing
Committee Member

The Graduate School has verified and approved the above-named committee members and certifies that the thesis has been approved in accordance with university requirements.

ACKNOWLEDGMENTS

We acknowledge the support from NASA grant 80NSSC22K0595. The IMERG dataset was provided by the NASA/Goddard Space Flight Center and PPS which developed and computed the IMERGE as a contribution to GPM and archived at the NASA GES DISC.

TABLE OF CONTENTS

List of Tables vi
List of Figures vii
Abstract x

1. INTRODUCTION 1

1.1 The Onset and Demise of the Rainy Season 2
1.2 Previous Studies 3
1.3 Objectives 5

2. DATA AND METHODS 6

2.1 Data 6
2.1.1 Rainfall Dataset 6
2.2.2 Climate Variables 7
2.2 Methods 7
2.2.1 Definition of Onset, Demise, Seasonal Length, and Seasonal Rain 7
2.2.2 Perturbation Method 9
2.2.3 Correlations with Climate Variables 10
2.2.4 Area Under the Relative Operating Characteristic Curve 10

3. RESULTS 12

3.1 Area Averaged Diagnosis 12
3.1.1 Climatology 13
3.1.2 Onset, Demise, Seasonal Length, and Seasonal Rain Correlations 15
3.1.3 ENSO Correlations 17
3.1.3 Atlantic Warm Pool Correlations 18
3.1.3 Eastern Pacific Warm Pool Correlations 19
3.1.6 Probabilistic Skill of Seasonal Outlook 20
3.2 Local Diagnosis 21
3.2.1 Climatology 22
3.2.2 Onset, Demise, Seasonal Length, and Seasonal Rain Correlations 24
3.2.3 ENSO Correlations 26
3.2.3 Atlantic Warm Pool Correlations 30
3.2.3 Eastern Pacific Warm Pool Correlations 32
3.2.6 Probabilistic Skill of Seasonal Outlook 35

4. CONCLUSIONS 38

4.1 Area Averaged Diagnosis 38
4.2 Local Diagnosis 38
4.3 Future Studies 39

References 41

Biographical Sketch 43

LIST OF TABLES

Table 1 Contingency table used to solve for the 'Hit Rate' and 'False Alarm Rate' 11

Table 2 The correlations between onset date (ON), demise date (DEM), seasonal length (LEN), and seasonal rain (RAIN) for a) Guatemala (GTM), b) Belize (BLZ), c) El Salvador (SLV), d) Honduras (HND), e) Nicaragua (NIC), f) Costa Rica (CRI), and g) Panama (PAN). The bold values are significant at a 95% confidence interval 16

Table 3 The correlation of ENSO index (Niño3.4 SSTA averaged over the JJA season and previous DJF season) for a) Guatemala (GTM), b) Belize (BLZ), c) El Salvador (SLV), d) Honduras (HND), e) Nicaragua (NIC), f) Costa Rica (CRI), and g) Panama (PAN). with Onset date (Od), Demise date (Dd), Length of the Season (LoS), and Seasonal Rain (SR) of the rainy season. The bold values are significant at a 95% confidence interval.. 17

Table 4 The correlation of the area, onset date, and demise date of the Atlantic Warm Pool for a) Guatemala (GTM), b) Belize (BLZ), c) El Salvador (SLV), d) Honduras (HND), e) Nicaragua (NIC), f) Costa Rica (CRI), and g) Panama (PAN). with Onset date (Od), Demise date (Dd), Length of the Season (LoS), and Seasonal Rain (SR). The bold values are significant at a 95% confidence interval. 18

Table 5 The correlation of the area, onset date, and demise date of the Eastern Pacific Warm Pool for a) Guatemala (GTM), b) Belize (BLZ), c) El Salvador (SLV), d) Honduras (HND), e) Nicaragua (NIC), f) Costa Rica (CRI), and g) Panama (PAN). with Onset date (Od), Demise date (Dd), Length of the Season (LoS), and Seasonal Rain (SR). The bold values are significant at a 95% confidence interval 20

LIST OF FIGURES

Figure 1 The 22-year (2001-2022) climatological seasonal cycle of rainfall area averaged over Guatemala (GTM), Belize (BLZ), El Salvador (SLV), Honduras (HND), Nicaragua (NIC), Costa Rica (CRI), and Panama (PAN) from the 12-h latency IMERG product 1

Figure 2 Isochrones of the mean date of the beginning of the rainy pentads are contoured. From Gramzow and Henry (1972) 4

Figure 3 Isochrones of the mean date of the end of the rainy pentads are contoured. From Gramzow and Henry (1972) 4

Figure 4 A schematic illustration of the time series of daily rainfall (blue bars; mm day^{-1}) and its corresponding cumulative daily anomaly curve (obtained from subtracting the annual mean climatological rainfall from the daily rain rate; green line; mm) over a specific grid point over Nicaragua for the year 2009. The onset (Julian Day: 111 (April 21)) and demise (Julian Day: 310 (November 6)) dates of the rainy season are indicated in the figure 8

Figure 5 The ensemble mean (EM) of 1001 members (solid black line) of the daily time series of precipitation over a specific grid point with the ensemble minimum and maximum (spread) shown in light red shade for the year 2009 9

Figure 6 Map of Central America showing the 7 countries in the study and the topography of the region. Map generated using ArcGIS online powered by ESRI 12

Figure 7 Box and whisker plots of (a) onset date (Julian Day), (b) demise date (Julian Day), (c) seasonal length (days), and (d) seasonal rain (mm) for a) Guatemala, b) Belize, c) El Salvador, d) Honduras, e) Nicaragua, f) Costa Rica, and g) Panama. The median value is indicated by the red line (approximately in the middle of the box) with the top and bottom edges of the box representing the 75^{th} and the 25^{th} percentile and the whiskers and dots representing the extreme data points of the ensemble spread and outliers (more than 1.5 times the inter-quartile range), respectively. The least squares fit line (black solid line) through the median value with the Sen's slope is also shown with three, two, and one asterisk indicating that the slope is significant at the 90%, 95%, and 99% confidence intervals, respectively. The units of the slope are a) Julian day per year, b) Julian day per year, c) day per year, d) mm per year 14

Figure 8 The area under the relative operating characteristic curve of the outlook for (a, b) seasonal length and (c,d) seasonal rain based on onset date variations for Guatemala (GTM), Belize (BLZ), El Salvador (SLV), Honduras (HND), Nicaragua (NIC), Costa Rica (CRI), and Panama (PAN) 21

Figure 9 The 22-year (2001-2022) climatological median (a) onset date (Julian Day), (b) demise date (Julian Day), (c) seasonal length (days), and (d) seasonal rain from 12h latency IMERG product... 22

Figure 10 The standard deviation of (a) onset date (days), (b) demise date (days), (c) length (days), and (d) seasonal rain (mm) of the wet season 24

Figure 11 The correlations of the onset date with anomalies of (a) demise date (b) length, and (c) seasonal rain. The statistically significant values at a 5% significance level according to the t-test are stippled black. The statistically significant values at a 1% significance level according to the t-test are stipple white. 25

Figure 12 The correlations of the demise date with anomalies of (a) length and (b) seasonal rain of the wet season. (c) The correlations of the seasonal length with corresponding seasonal rainfall anomalies of the wet season. The statistically significant values at a 5% significance level according to the t-test are stippled black. The statistically significant values at a 1% significance level according to the t-test are stipple white... 26

Figure 13 The correlations of the DJF (-1) Nino3.4 SST index (OISSTv2; Reynolds et al. 2002) with anomalies of (a) onset date, (b) demise date, (c) seasonal length, and (d) seasonal rain of the rainy season. The statistically significant values at a 5% significance level according to the t-test are stippled black. The statistically significant values at a 1% significance level according to the t-test are stippled white... 27

Figure 14 The correlations of the MAM Nino3.4 SST index (OISSTv2; Reynolds et al. 2002) with anomalies of (a) onset date, (b) demise date, (c) seasonal length, and (d) seasonal rain of the rainy season. The statistically significant values at a 5% significance level according to the t-test are stippled black. The statistically significant values at a 1% significance level according to the t-test are stippled white. 28

Figure 15 The correlations of the JJA Nino3.4 SST index (OISSTv2; Reynolds et al. 2002) with anomalies of (a) onset date, (b) demise date, (c) seasonal length, and (d) seasonal rain of the rainy season. The statistically significant values at a 5% significance level according to the t-test are stippled black. The statistically significant values at a 1% significance level according to the t-test are stippled white..... 29

Figure 16 The correlations of the Atlantic Warm Pool onset date (Misra et al. 2014; OISSTv2; Reynolds et al. 2002) anomalies of (a) onset date, (b) demise date, (c) seasonal length, and (d) seasonal rain of the rainy season. The statistically significant values at a 5% significance level according to the t-test are stippled black. The statistically significant values at a 1% significance level according to the t-test are stippled white 30

Figure 17 The correlations of the Atlantic Warm Pool demise date (Misra et al. 2014; OISSTv2; Reynolds et al. 2002) anomalies of (a) onset date, (b) demise date, (c) seasonal length, and (d) seasonal rain of the rainy season. The statistically significant values at a 5%

significance level according to the t-test are stippled black. The statistically significant values at a 1% significance level according to the t-test are stippled white 31

Figure 18 The correlations of the Atlantic Warm Pool area (Misra et al. 2014; OISSTv2; Reynolds et al. 2002) anomalies of (a) onset date, (b) demise date, (c) seasonal length, and (d) seasonal rain of the rainy season. The statistically significant values at a 5% significance level according to the t-test are stippled black. The statistically significant values at a 1% significance level according to the t-test are stippled white 32

Figure 19 The correlations of the Eastern Pacific Warm Pool onset date index (Misra et al. 2016; OISSTv2; Reynolds et al. 2002) with anomalies of (a) onset date, (b) demise date, (c) seasonal length, and (d) seasonal rain of the rainy season. The statistically significant values at a 5% significance level according to the t-test are stippled black. The statistically significant values at a 1% significance level according to the t-test are stippled white... 33

Figure 20 The correlations of the Eastern Pacific Warm Pool demise Date index (Misra et al. 2016; OISSTv2; Reynolds et al. 2002) with anomalies of (a) onset date, (b) demise date, (c) seasonal length, and (d) seasonal rain of the rainy season. The statistically significant values at a 5% significance level according to the t-test are stippled black. The statistically significant values at a 1% significance level according to the t-test are stippled white... 34

Figure 21 The correlations of the Eastern Pacific Warm Pool area index (Misra et al. 2016; OISSTv2; Reynolds et al. 2002) with anomalies of (a) onset date, (b) demise date, (c) seasonal length, and (d) seasonal rain of the rainy season. The statistically significant values at a 5% significance level according to the t-test are stippled black. The statistically significant values at a 1% significance level according to the t-test are stippled white... 35

Figure 22 The area under the Relative Operating Characteristic (ROC) curve for the outlook of a) a longer wet season based on early onset, b) a wetter wet season based on early onset, c) a shorter wet season based on later onset, and d) drier wet season based on later onset of the wet season. Only regions with an area under the ROC curve ≥ 0.5, which signifies probabilistic skill that is better than random forecast are shaded 37

ABSTRACT

Central America exhibits a distinct seasonal cycle of rainfall, which is objectively defined in this study as having an onset date and a demise date of the wet season on the first and the last day of the year when its daily rainfall exceeds and falls below the annual mean rainfall climatology, respectively. This is defined at both a regional scale and the granularity of the rainfall analysis dataset. Additionally, the methodology diagnoses the onset/demise dates of the wet season from an ensemble of 1000 members per season by perturbing the original time series to obtain robust probabilistic estimates. The variations in the onset date, demise date, seasonal length, and seasonal rain are considered with the variations of the El Niño Southern Oscillation, the Atlantic Warm Pool, and the Eastern Pacific Warm Pool to better understand the influences of these large-scale climate variations. Our analysis reveals that these external factors have relatively less influence on the variations of the evolution of the wet season over Central America. It is shown that both onset and demise date variations have a bearing on the seasonal length and seasonal rainfall anomaly but impact them independently of each other. This study demonstrates that a seasonal outlook based solely on the onset date variations has useful prediction skills that portend for real-time monitoring of the onset date of the wet season.

CHAPTER 1

INTRODUCTION

Central America, comprising of Belize, Guatemala, El Salvador, Honduras, Nicaragua, Costa Rica, and Panama, is an isthmus bridging North and South America. This region does not exhibit much seasonal variation in terms of temperatures. The traditional four seasons do not bear much insight into the climate of the countries of Central America. Instead, Central America is said to have two seasons: a dry season and a wet season. This distinct seasonal cycle of rainfall is recognized as the Central American monsoon which also serves as a bridge for a unified view of the North and the South American Monsoon systems (Vera et al. 2006). The dramatic shift of the seasons can be seen in Figure 1 where the climatological seasonal cycle of rainfall area averaged over each country in the region for the years 2001-2022 is plotted. The rainy season begins around April or May and lasts until about November. The evolution of the rainy season proves to be rather heterogeneous given the region's complex geography (e.g., a narrow isthmus oriented northwest-southeast direction, surrounded by relatively warm oceans), topography, and the vicinity of oceanic Inter Tropical Convergence Zone (ITCZ). For example, the region's

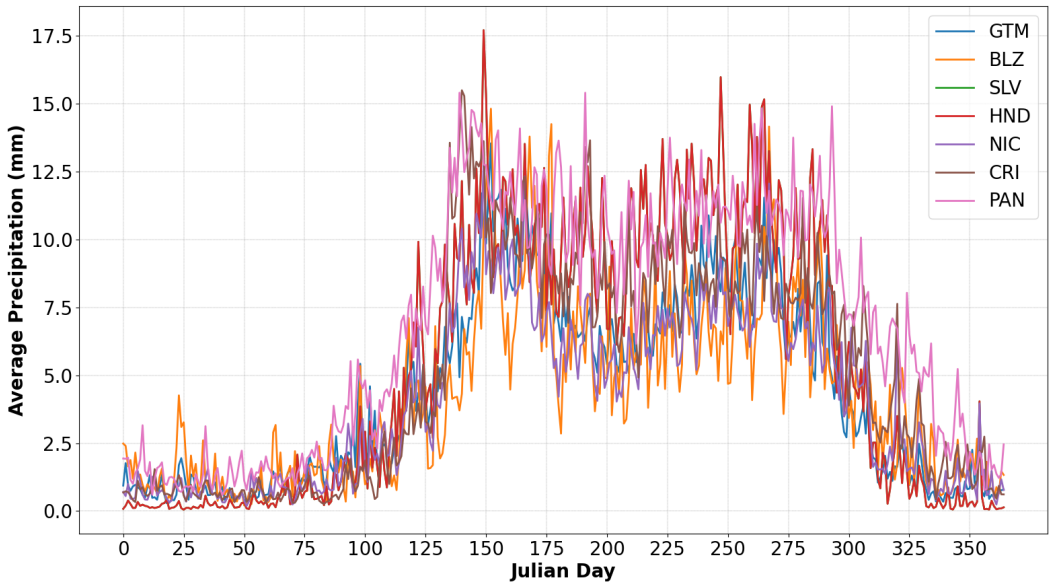

Figure 1: The 22-year (2001-2022) climatological seasonal cycle of rainfall area averaged over Guatemala (GTM), Belize (BLZ), El Salvador (SLV), Honduras (HND), Nicaragua (NIC), Costa Rica (CRI), and Panama (PAN) from the 12-h latency IMERG product.

complex topography in the narrow isthmus and its interaction with the seasonally varying easterly trade winds gives rise to a differing seasonal precipitation cycle between its Pacific and Caribbean slopes (Magana et al. 1999; Alfaro 2002; Taylor and Alfaro 2005; Amador et al. 2006). Furthermore, the north-south contrast in the rainy seasons from Panama to Belize is also distinct owing partly to the movement and extent of the ITCZ and its associated circulations and the strength and extent of the subtropical highs in the Pacific and the Atlantic Oceans. Additionally, the variability of the regional climate system forced by external factors like the El Niño Southern Oscillation (ENSO), tropical North Atlantic sea surface temperatures (SSTs), and internal chaotic variations make anticipating or forecasting the seasonal hydroclimate over the region a challenging task (Alfaro et al. 2017; Kowal et al. 2023). A further complication is the presence of the midsummer drought, which is a relative minimum of rainfall that occurs in the middle of the wet season, resulting in a bimodal peak of rainfall as can be seen in Figure 1 (Alfaro et al. 2017; Gramzow and Henry 1972; Magana et al. 1999). It should be noted that our methodology ignores the mid-summer drought phenomenon. Although significant importance is attached separately to the variations of the primary peak (May-June) and secondary maximum (September-October) of rainfall (Magana et al. 1999; Alfaro et al. 2017), there is still significant rainfall during the July-August period of the "canicular" (> 5 mm day^{-1}; Figure 1) to broadly include it as part of the wet season.

The exact timing, length, and severity of these rainy seasons are crucial to the economy of Central America and all those regions that rely on their agricultural imports (Alfaro et al. 2017; Kowal et al. 2023; Magana et al. 2019). Further, Central America is a popular tourist destination which is heavily influenced by the timing of the rainy season. Therefore, researching the onset and demise of the rainy season over Central America is significant. More commonly, seasons with fixed calendar months are used in climate analysis (e.g., Vera et al. 2006; Alfaro et al. 2017). However, it is easily conceivable to think of seasons with varying seasonal lengths based on variations of the onset and demise dates of the season if they are diagnosed objectively.

1.1 The Onset and Demise of the Wet Season

There is no standard definition to diagnose the onset or demise of the wet season over Central America. The variety of methods includes using station data to define rainy pentads thresholds (Alfaro 2002; Gramzow and Henry 1972; Nakegawa et al. 2015), using Global

Climate Models, statistical methods based on observed SST values, or a hybrid (Kowal et al. 2023).

The implementation of the onset and demise diagnosis used in this study has been previously used in other tropical regions exhibiting a strong seasonality of rainfall (Liebmann and Marengo 2001; Misra and DiNapoli 2014; Dunning et al. 2016; Uehling and Misra 2020). The onset and demise are defined as the day the cumulative anomaly of rainfall reaches its minimum and maximum, respectively. This methodology has the advantage of being dependent solely on rainfall, which is a readily available variable. Further, this methodology is not easily susceptible to false onsets. Also, by having an onset and demise date that vary each year, the correlations between the onset, demise, length of the rainy season, and amount of rainfall during the rainy season can be determined. These correlations may serve a purpose by suggesting that onset date variations can be used to predict the severity and duration of the rainy season.

1.2 Previous Studies

Gramzow and Henry (1972) made the first comprehensive study of the rainy season of Central America. They acquire daily rain data from 124 stations in Central America with the number of years of records ranging from 2 to 20 years. Then, the daily data was grouped into 5-day totals. The start of the rainy season is defined in their study as the days when the mean of the rainy pentad reaches a threshold of 25mm, which corresponds with an estimated amount of rain from one mesoscale rainstorm. Similarly, the end of the rainy season is the last pentad reaching the 25mm threshold. Using an average of these dates and the station locations, isochrone maps were created (Figures 2 and 3). It should be noted that their maps do not include Belize and Guatemala.

As seen in Figure 2, Gramzow and Henry (1972) found that the start of the rainy season begins around April 11th, along the southern part of the Caribbean coast of Panama and Costa Rica. The rainy season next begins through Panama and Costa Rica and moves inland from the east coast of Nicaragua. Simultaneously the mountains of northern El Salvador also experience the start of the season. This start in the mountains occurs before the arrival of the northward progressing isochrones. Gramzow and Henry (1972) suggest orographic lift causes this early start in the mountainous region. The last region to experience the start of the rainy season is the northern coast of Honduras and a small region north of Lake Nicaragua around late June.

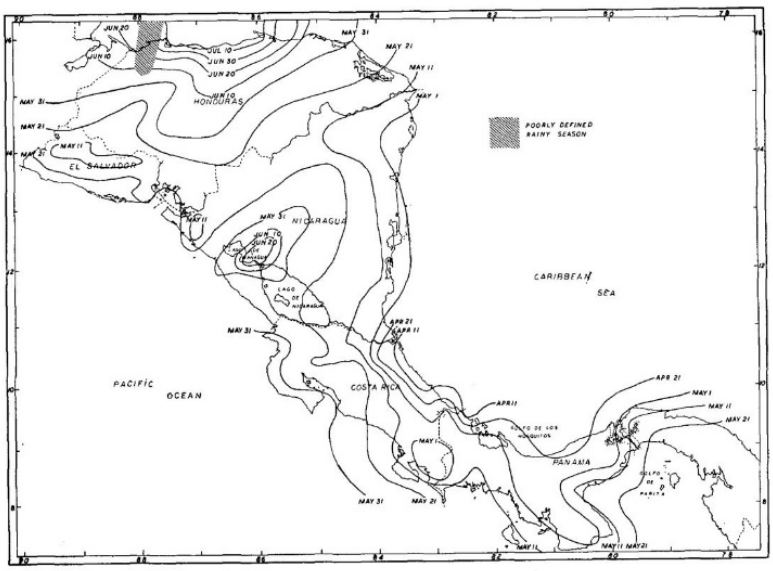

FIG. 3. Mean date of beginning of the rainy pentads.

Figure 2: Isochrones of the mean date of the beginning of the rainy pentads are contoured. From Gramzow and Henry (1972).

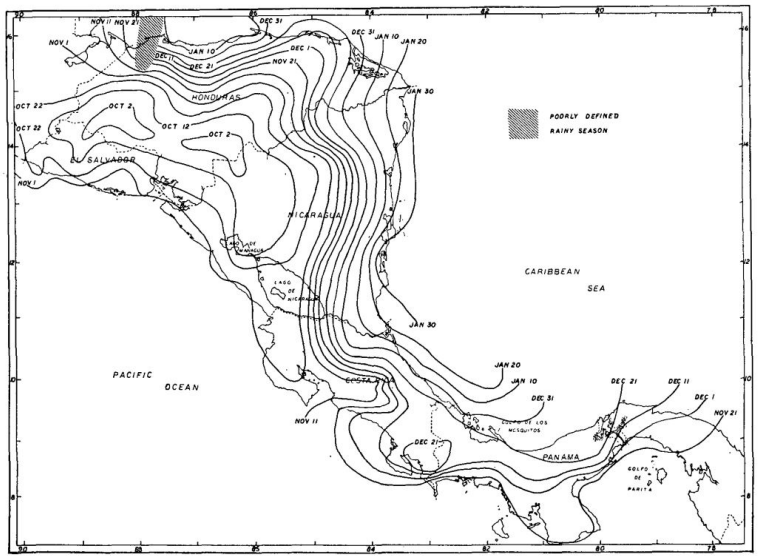

FIG. 6. Mean date of end of the rainy pentads.

Figure 3: Isochrones of the mean date of the end of the rainy pentads are contoured. From Gramzow and Henry (1972).

The retreat of the rainy season following Gramzow and Henry (1972), as shown in Figure 3, begins in early October near the mountains of El Salvador, Honduras, and Nicaragua. The retreat continues southward, though preferring an earlier end along the Pacific coast as opposed to the Caribbean coast. The final region to experience the end of the rainy season is along the northern coast of Honduras and the eastern coast of Nicaragua as late as January 30th.

Gramzow and Henry (1972) conclude that though these patterns can be discerned, their detailed analysis is limited by the scarcity and short length of rainfall data.

Alfaro (2000) is another comprehensive study of the annual cycle of rainfall over Central America. The daily rain data from 94 rain gauges in Central America were used to define the start and the end date of the rainy season. Similar to Gramzow and Henry (1972), Alfaro (2000) split the data into pentads of accumulated rainfall. The start date was defined as the first pentad with at least 25mm of accumulated rainfall that also has at least one of the two pentads surrounding or after also exceeding this minimum threshold. Alfaro (2000) found the average start date of the wet season was around mid-May. Alfaro (2000) found, like Gramzow and Henry (1972), that the earliest start dates of the rainy season were in the South and the later start date values were in the North. The reverse was seen for the end dates, where the average end date is around mid-November. Overall, Alfaro's study concluded that this latitudinal dependence found in the start and end dates of the rainy season could be partially explained by the seasonal migration of the ITCZ (which is associated with instability and humidity convergence), the annual cycle of the trade winds that weaken during the rainy season (allowing mesoscale systems to develop), and by the annual cycle of the total radiation at the top of the atmosphere which has the highest values during the rainy season (Alfaro, 2000).

1.3 Objectives

Following the previous studies utilizing the definition of the onset and demise of a rainy season (Liebmann and Marengo 2001; Misra and DiNapoli 2014; Dunning et al. 2016; Uehling and Misra 2020), this study first intends to characterize the variations of the seasonal onset, demise, length, and rain of the wet season over Central America. With a clearer picture of the seasonal variations, this study secondly intends to provide a method of using the declaration of the onset date to predict the seasonal length and rainfall.

CHAPTER 2

DATA AND METHODS

2.1 Data

The methodology used in this study follows the previous studies utilizing the cumulative anomaly of rainfall as discussed in Section 1 (Liebmann and Marengo 2001; Misra and DiNapoli 2014; Dunning et al. 2016; Uehling and Misra 2020). Therefore, the only variable necessary to define the onset and demise of the wet season is rainfall. This study uses both an area-averaged approach to examine the varying onset and demise dates for each country in Central America and a local approach where these dates are computed at the native resolution of the rainfall analysis.

2.1.1 Rainfall Dataset

National Aeronautics and Space Administration's (NASA) Integrated Multi-Satellite Retrievals for Global Precipitation Mission version 6 (IMERG) rainfall data is the primary data set used for this study. This data comes from the Global Precipitation Measurement (GPM) mission launched in 2014 and developed by NASA and the Japanese Aerospace Exploration Agency (JAXA). The IMERG dataset uses an algorithm to combine the Tropical Rainfall Measuring Mission (TRMM) precipitation estimates for 2000-2015 with the IMERG precipitation estimates for 2014-present, resulting in a dataset running from June 2000 to the present. This dataset is available at half-hour temporal resolution with 0.1° grid spacing. The IMERG rainfall analysis products include Early, Late, and Final Run which have a latency of ~ 4 hours, 12 hours, and 3.5 months, respectively. The latency stems from the discrete frequency at which the data is downloaded, the use of algorithms to convert observed radiance to precipitation, and the availability and use of numerical forecasts and reanalysis (Misra et al. 2022). The Early Run, for example, uses the forward propagation morphing technique, which produces a rainfall analysis approximately 4 hours after the observation time of the radiance. Similarly, the late run of IMERG includes in addition to forward, backward propagation morphing preprocessing. This requires that the analysis has to wait for the following microwave overpass to occur to initiate the backward propagation morphing step to derive precipitation from the microwave data. The Late Run has a latency of 3.5 months because it additionally uses Modern-Era Retrospective Analysis for Research and Applications, version 2 (MERRA2; Gelaro

et al. 2017), monthly rain gauge analysis dataset (Schneider et al. 2017), and the revised precipitation retrievals that use ERA-5 (Hersbach et al. 2019), and ERA-Interim (Dee et al. 2011) reanalysis. Since the current project has potential real-time applications, the Late Run product is used. The real-time monitoring of the evolution of the rainy season, however, requires us to wait a week to 10 days after the onset of the season to confirm its occurrence. Similarly, we have to wait a week to 10 days after the demise of the season. Therefore, the 12-hour latency of the Late Run product of IMERG is tolerable for this work. Furthermore, Misra et al. (2022) showed that the Late Run, for the applications of this study, has comparable fidelity to the Final Run of IMERG (Misra et al. 2022).

2.1.2 Climate Variables

In an attempt to better understand the forcings and influences of the Central American rainy season, the correlations between various climate variables and the Central American rainy season are examined. Special consideration is given to ENSO. The Optimally Interpolated SST v2 (OISSTv2; Reynolds et al. 2002) is used to develop the Niño3.4 SST index. This index is separated into December, January, February (DJF), March, April, May (MAM), and June, July, August (JJA). The previous year's DJF (DJF-1) is used when accessing the correlations.

Considering the intimate proximity of Central America to both the Atlantic Warm Pool and the Eastern Pacific Warm Pool, these are also used in the study. OISSTv2 was similarly used to define the area, onset, and demise of the Atlantic Warm Pool and the Eastern Pacific Warm Pool following Misra et al. (2014) and Misra et al. (2016), respectively.

2.2 Methods

2.2.1 Definition of Onset, Demise, Seasonal Length, and Seasonal Rain

The onset and the demise dates of the rainy season are defined as the first and the last days of the year when the daily rain rate exceeds and falls below the climatological annual mean rainfall rate. The two equations used are:

$$C'_m(i) = \sum_{n=1}^{i} \left[A_m(n) - \bar{\bar{C}}\right] \text{----------(1)}$$

$$\bar{\bar{C}} = \frac{1}{MN} \sum_{m=1}^{M} \sum_{n=1}^{N} A(m,n) \text{----------(2)}$$

Where $\bar{\bar{C}}$ is the climatology of the annual mean of the rainfall over N(=365/366) days for M years, C'_m is the cumulative anomaly for day i of year m, $A_m(n)$ is the rainfall for day n of year m. The onset date is thus when the daily cumulative anomaly is at its minimum, and the demise date is when the daily cumulative anomaly is at its maximum for the year. The seasonal length is then defined as the number of days between the onset date and the demise date. The seasonal rain is found by summing the daily rainfall between the onset date and demise date. The cumulative anomaly curve and daily rainfall of a grid point over Nicaragua can be seen in Figure 4 which shows the characteristic curve and its season encapsulation.

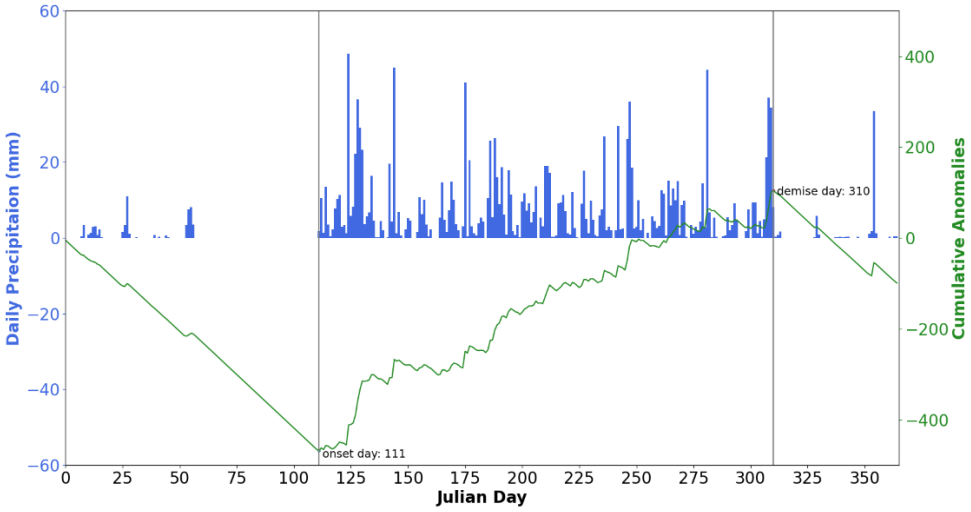

Figure 4: A schematic illustration of the time series of daily rainfall (blue bars; mm day^{-1}) and its corresponding cumulative daily anomaly curve (obtained from subtracting the annual mean climatological rainfall from the daily rain rate; green line; mm) over a specific grid point over Nicaragua for the year 2009. The onset (Julian Day: 111 (April 21)) and demise (Julian Day: 310 (November 6)) dates of the rainy season are indicated in the figure.

This method can be applied over a regional scale where a region, or in the case of this study, a country's rainfall is area averaged to solve for the onset date, demise date, seasonal length, and seasonal rainfall. Further, this method can also be applied to individual grid points of the rainfall analysis and mapped to show finer details in the evolution of the wet season. Both applications will be examined in this study of Central America.

To ensure the cumulative anomaly's minimum and maximum occur at a reasonable time of the year, a window of acceptable dates is created. There are a few years where the rainfall

over the rainy season is not significant enough to make the cumulative anomaly positive. This results in the demise date occurring on the first day of the year, which is unrealistic. Creating the window resolves this issue. The reasonable dates are defined using a 30-day window with the median onset/demise date at the center of the regional scheme. On the grid point scale, the windows were defined as the span of the windows for all the countries in Central America. As a result, the window for onsets is between Julian day 96 and 150, and the window for demises is between Julian day 279 and 346.

2.2.2 Perturbation Method

A perturbation method is implemented to help account for the uncertainty in the rainfall data. Furthermore, to reduce the chances of random synoptic or mesoscale events that are not connected to the seasonal cycle influencing the diagnosis of the onset/demise date of the rainy season, a perturbation method akin to a bootstrapping is implemented (Misra et al. 2023). The perturbation method involves shuffling the original daily time series of rainfall on the timescale of 6 days (~synoptic scale). In addition to shuffling, the daily rain rates of some randomly chosen days within the sequence of the 3 days of the chosen date are replaced. The perturbation is conducted 1000 times for each daily time series of rainfall. Consequently, an ensemble of onset/demise dates is generated from this 1001 time series. For some of the deterministic analyses conducted in this study, the median of onset/demise from the ensemble of 1001 iterations (1000 perturbed time series plus the original time series) is used. The ensemble spread can be seen in Figure 5.

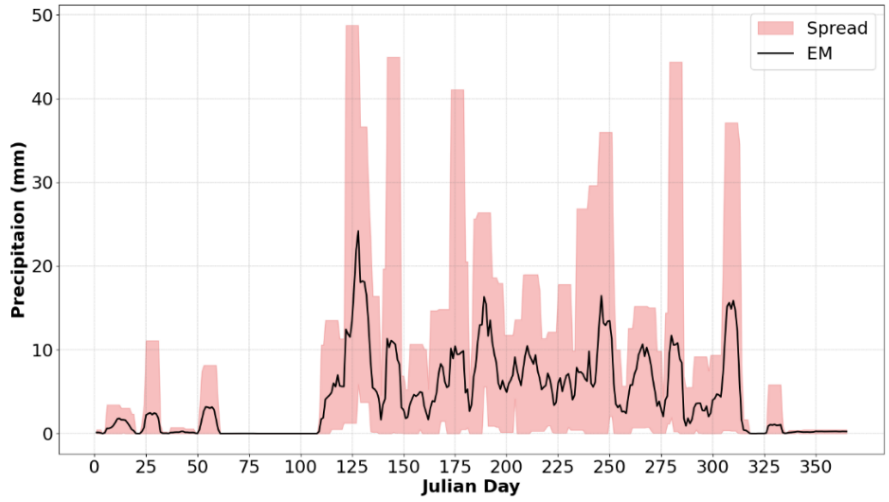

Figure 5: The ensemble mean (EM) of 1001 members (solid black line) of the daily time series of precipitation over a specific grid point with the ensemble minimum and maximum (spread) shown in light red shade for the year 2009.

2.2.3 Correlations with Climate Variables

To evaluate the strength of the linear correlation between large-scale climate variables and the onset date, demise date, seasonal length, and seasonal rain, the Pearson correlation is used. The significance is determined using a t-test.

2.2.4 Area Under the Relative Operating Characteristic Curve

To assess the forecasting skill of onset date on the seasonal length and seasonal rain, the area under the relative operating characteristic curve is used following Graham et al. (2000), Misra (2004), and Narosky and Misra (2021). The relative operating characteristic (ROC) curve is a plot of the hit rate vs the false alarm rate at varying thresholds. The area under the ROC curve (AROC) then summarizes the performance of the variable in discriminating between a correct or an incorrect forecast. In this study, an early/late onset date is used to forecast whether the season will be long/short and wetter/dryer. The 1000 onset date iterations developed in the perturbation process are used to form the ROC curve.

To create the ROC curve, the seasonal lengths and seasonal rains are separated into terciles to determine if the year experienced a long, normal, or short season length and a wetter, normal, or dryer season. Further, the onset dates are split into terciles as well to determine if the onset date is early, normal, or late. Using the onset terciles, the 1000 iterations per year are separated to count how many iterations showed an early, normal, or late-onset date. To solve for the Hit Rate (HR) and False Alarm Rate (FAR) needed to plot the ROC curve, 11 contingency tables are created (table 1). The ‘event’ in the table is the long wet season, short wet season, wetter wet season, or dryer wet season. The ‘ensemble probability’ is the fraction of ensemble members that determined an early or late onset. The probability thresholds used to compute ROC range from 0% to 100% increasing by 10% increments.

To fill the contingency tables, each year is examined. If the event occurred in that year, the percentage of ensemble members that correctly predicted the event is calculated. If the ensemble percentage exceeds the threshold percentage, the result is a ‘Hit’ (H). If the ensemble percentage does not exceed the threshold percentage, the result is a ‘Miss’ (M). If the event does not occur that year, the percentage of onset iterations that incorrectly predicted the event is solved. If the ensemble percentage exceeds the threshold percentage, the result is a ‘False Alarm’

(FA). If the ensemble percentage does not exceed the threshold percentage, the result is a 'Correct Rejection' (CR). This is repeated for all thresholds and all years. Finally, the H, M, FA, and CR in each table are summed for each table. At each percentage, the HR and FAR are solved using the following two equations:

$$HR=H/(H+M) \text{ ----------(1)}$$

$$FAR=FA/(FA+CR) \text{ ----------(2)}$$

The HR is plotted against the FAR to create the ROC curve. The area under the curve is then solved using the trapezoidal method to result in the ROC AUC score. This process is repeated for all events (early onset with longer season, early onset with wetter season, late onset with shorter season, and late onset with dryer season) to create four ROC curve plots.

A ROC AUC score below indicates the ensemble has no more skill than random chance. A ROC AUC score of 0.5 to 1 indicates the ensemble has predictability, with a score of 1 resulting from the ensemble predicting the correct event every time.

	Ensemble probability for the event exceeds the threshold	Ensemble probability for the event does not exceed the threshold
Event is observed	Hit (H)	Miss (M)
Event is not observed	False Alarm (FA)	Correct Rejection (CR)

Table 1: Contingency table used to solve for the 'Hit Rate' and 'False Alarm Rate'.

CHAPTER 3

RESULTS

3.1 Area Averaged Diagnosis

As a first step, an analysis of the area averaged regions of the seven countries in Central America (Guatemala, Belize, El Salvador, Honduras, Nicaragua, Costa Rica, and Panama) was conducted (Figure 6). The onset and demise of the rainy season are defined based on area-averaged rainfall for these seven countries. The results in the following sub-sections pertain to these area-averaged values.

Figure 6: Map of Central America showing the 7 countries in the study and the topography of the region. Map generated using ArcGIS online powered by ESRI.

3.1.1 Climatology

Figure 7 shows the box and whisker plots of the ensemble of the 1001 diagnosed onset dates, demise dates, seasonal length, and seasonal rain for each country in Central America. The Sen's slope is indicated in each plot with three, two, and one asterisk indicating if the slope is significant at the 90%, 95%, and 99% confidence interval, respectively.

Consistent with earlier studies, the onset date usually occurs on average over all of Central America around Julian Day 130 (~May 10) (Figure 7a). Geographically, the southernmost country, Panama, typically has the earliest onset date with an average of Julian day 124 (~May 4). Belize, the northernmost country in Central America, typically exhibits the latest onset date with an average of Julian day 135 (~May 15). This suggests the wet season progresses from South to North. While the slopes are generally small in Figure 7a, Costa Rica does display a positive slope significant at the 95% confidence interval. Though Costa Rica is the only country with a statistically significant slope, the three southernmost countries (Nicaragua, Costa Rica, and Panama) all have a positive slope. This suggests the onset dates are occurring later in the year than previously in those countries.

Figure 7b displays the box plots of the rainy season's demise dates. The demise date occurs on average over all of Central America around Julian day 300 (~October 27). The northernmost countries, Guatemala and Belize, typically have the earliest demise dates with an average of Julain day 295 (~October 22). Panama, the southernmost country in Central America, typically exhibits the latest demise date with an average of Julian day 304 (~October 31). This suggests the end of the wet season progresses from North to South, opposite of the onset of the wet season. All of the countries except Guatemala and Belize have a negative slope. Costa Rica's negative slope is significant at the 90% confidence interval and Panama's negative slope is significant at the 95% confidence interval. This suggests that the demise date is occurring earlier than previously in those countries.

The average seasonal length in Central America is 170 days (Figure 7c). The northernmost country (Belize) experiences the shortest average seasonal length at 162 days, and the southernmost country (Panama) has the longest average seasonal length at 181 days. This makes sense given the seasonal progression derived from Figures 7a-b. Similar to the slopes of the demise dates, all of the countries except Guatemala and Belize have a negative slope with Costa Rica's slope significant at the 95% confidence interval and Panama's slope significant at

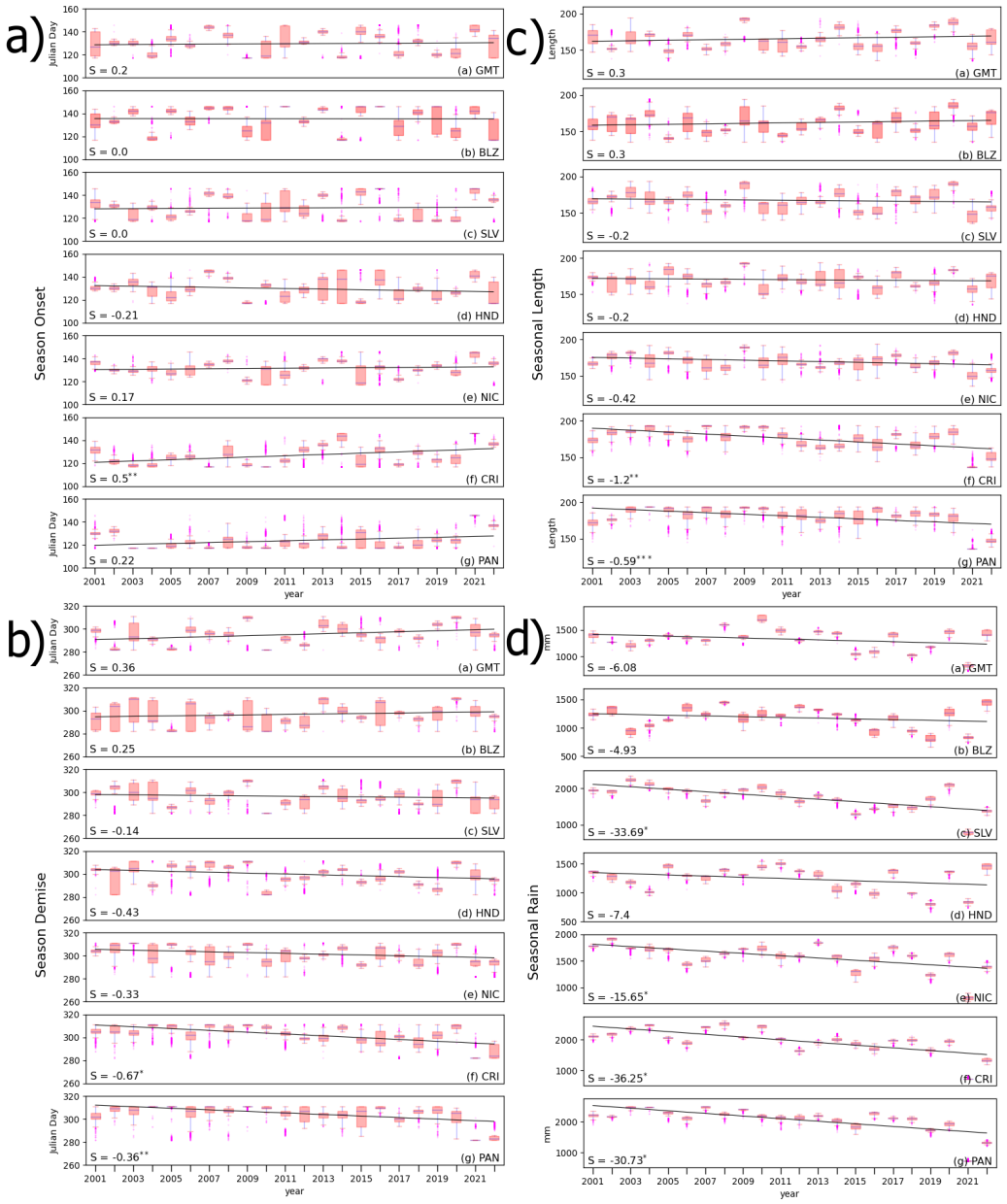

Figure 7: Box and whisker plots of (a) onset date (Julian Day), (b) demise date (Julian Day), (c) seasonal length (days), and (d) seasonal rain (mm) for a) Guatemala, b) Belize, c) El Salvador, d) Honduras, e) Nicaragua, f) Costa Rica, and g) Panama. The median value is indicated by the red line (approximately in the middle of the box) with the top and bottom edges of the box representing the 75th and the 25th percentile and the whiskers and dots representing the extreme data points of the ensemble spread and outliers (more than 1.5 times the inter-quartile range), respectively. The least squares fit line (black solid line) through the median value with the Sen's slope is also shown with

the 99% confidence interval. These slopes follow the slopes of Figure a-b in the sense that a later onset and an earlier demise date would result in a shorter seasonal length. These relationships are explored more in Table 2.

The average amount of seasonal rain in Central America is around 1590mm (Figure 7d). The northernmost country (Belize) experiences the lowest average seasonal rain at around 1181mm, and the southernmost country (Panama) experiences the highest average seasonal rain at around 2075mm. This similarly makes sense as a longer season would typically experience more rainfall. All of the countries have a negative slope, suggesting there is less rainfall per season. El Salvador, Nicaragua, Costa Rica, and Panama all have a negative slope statistically significant at the 99% confidence interval.

3.1.2 Onset, Demise, Seasonal Length, and Seasonal Rain Correlations

Table 2 shows the correlations between the onset date, demise date, seasonal length, and seasonal rain for each country. The values in bold are significant at the 95% confidence interval according to the t-test. The onset and demise dates have a statistically significant correlation with the seasonal length for all countries, implying with an earlier onset, the season will be longer, and with a later onset, the season will be shorter. With an earlier demise date, the season will be shorter, and with a later demise date, the season will be longer. Further, the onset and demise dates also have some significant correlations with seasonal rain (Nicaragua, Costa Rica, and Panama), but not for all countries (Guatemala, Belize, El Salvador, and Honduras). This implies that for regions with statistically significant correlations, with an earlier onset of the season, the season will be wetter, and with a later onset, the season will be dryer. Also, with an earlier demise date, the season will be dryer, and with a later demise date, the season will be wetter. It follows that the diagnosis of the onset date may provide valuable insight into the season length and amount of rain. The demise, though demonstrating a strong correlation, serves no forecasting benefit since it can only be diagnosed after the season has ended. The correlations between the onset date and the demise date are insignificant for all countries except Costa Rica and Panama where a statistically significant negative correlation is present. This implies that in the majority of Central American countries, the variations of the onset and demise dates of the rainy season are independently influencing the seasonal rain and length of the rainy season variations. In Costa Rica and Panama, the negative correlations suggest that early and later onset seasons are

associated with later and early demise seasons, respectively. The correlations between the seasonal length and seasonal rain are generally positive (with the exceptions in Guatemala and Belize), with a longer or shorter season yielding a wetter or drier season, respectively. The relationship between the length of the season and seasonal rain becomes stronger for the southernmost countries in Central America (e.g., Costa Rica and Panama).

		Onset Date	Demise Date	Seasonal Length	Seasonal Rain
GTM	ON	1	-0.22	**-0.79**	-0.39
	DEM	-0.22	1	**0.76**	-0.01
	LEN	**-0.79**	**0.76**	1	0.26
	RAIN	-0.39	-0.01	0.26	1
BLZ	ON	1	0.11	**-0.76**	0.35
	DEM	0.11	1	**0.51**	0.05
	LEN	**-0.76**	**0.51**	1	0.2
	RAIN	0.35	0.05	0.2	1
SLV	ON	1	-0.02	**-0.66**	-0.28
	DEM	-0.02	1	**0.64**	0.34
	LEN	**-0.66**	**0.64**	1	**0.47**
	RAIN	-0.28	0.34	**0.47**	1
HND	ON	1	0.14	**-0.66**	-0.28
	DEM	0.14	1	**0.64**	0.34
	LEN	**-0.66**	**0.64**	1	**0.47**
	RAIN	-0.28	0.34	**0.47**	1
NIC	ON	1	-0.19	**-0.77**	-0.33
	DEM	-0.19	1	**0.77**	**0.43**
	LEN	**-0.77**	**0.77**	1	**0.52**
	RAIN	-0.33	**0.43**	**0.52**	1
CRI	ON	1	**-0.59**	**-0.9**	**-0.68**
	DEM	**-0.59**	1	**0.88**	**0.85**
	LEN	**-0.9**	**0.88**	1	**0.85**
	RAIN	**-0.68**	**0.85**	**0.85**	1
Pan	ON	1	**-0.78**	**-0.93**	**-0.83**
	DEM	**-0.78**	1	**0.85**	**0.87**
	LEN	**-0.93**	**0.85**	1	**0.9**
	RAIN	**-0.83**	**0.87**	**0.9**	1

Table 2: The correlations between onset date (ON), demise date (DEM), seasonal length (LEN), and seasonal rain (RAIN) for a) Guatemala (GTM), b) Belize (BLZ), c) El Salvador (SLV), d) Honduras (HND), e) Nicaragua (NIC), f) Costa Rica (CRI), and g) Panama (PAN). The bold values are significant at 95% confidence interval.

3.1.3 ENSO Correlations

Table 3 shows the correlations between the Niño 3.4 SST index for the previous years' December January February (DJF (-1)), March April May (MAM), and June July August (JJA) with the onset date, demise date, seasonal length, and seasonal rain of the wet season for each country in Central America. The bold values are significant at the 95% confidence interval according to the t-test. The majority of the correlations in Table 3 are statistically insignificant, suggesting that the influence of ENSO on these metrics is weak. However, the correlations of JJA Niño 3.4 SST index with seasonal rain over Guatemala and the onset date of the rainy season over Honduras are significant (with warm or cold ENSO events leading to a drier or wetter season over Guatemala and a later or earlier onset over Nicaragua, respectively). Similarly, the MAM Niño 3.4 SST index is significantly correlated with seasonal rain over Belize and demise date over Panama. Lastly, the preceding DJF Niño 3.4 SST index is positively correlated with the length of the season over Panama, suggesting warm or cold ENSO events are associated with a longer or shorter rainy season.

		DJF (-1) Niño3.4 SST	MAM Niño3.4 SST	JJA Niño3.4 SST
GTM	Od	-0.056	-0.251	-0.080
	Dd	-0.194	-0.024	0.033
	LoS	-0.097	0.138	0.075
	SR	-0.129	-0.160	**-0.449**
BLZ	Od	0.212	0.192	0.050
	Dd	0.126	0.134	-0.090
	LoS	0.039	0.064	-0.157
	SR	-0.419	**-0.453**	-0.204
SLV	Od	0.007	-0.130	-0.097
	Dd	-0.294	-0.187	0.166
	LoS	-0.152	0.028	0.173
	SR	0.121	0.022	-0.076
HND	Od	0.122	-0.095	-0.377
	Dd	-0.266	-0.288	0.013
	LoS	-0.262	-0.117	0.303
	SR	-0.258	-0.365	-0.313
NIC	Od	-0.199	-0.339	**-0.472**
	Dd	0.150	0.202	0.043
	LoS	0.260	0.374	0.326
	SR	0.060	0.022	-0.066
CRI	Od	-0.355	-0.296	-0.220
	Dd	0.172	0.204	0.103
	LoS	0.324	0.296	0.164
	SR	0.182	0.073	-0.001
Pan	Od	-0.403	-0.340	0.033
	Dd	0.417	**0.448**	0.308
	LoS	**0.437**	0.419	0.150
	SR	0.265	0.164	0.064

Table 3: The correlation of ENSO index (Niño3.4 SSTA averaged over the JJA season and previous DJF season) for a) Guatemala (GTM), b) Belize (BLZ), c) El Salvador (SLV), d) Honduras (HND), e) Nicaragua (NIC), f) Costa Rica (CRI), and g) Panama (PAN). with Onset date (Od), Demise date (Dd), Length of the Season (LoS), and Seasonal Rain (SR) of the rainy season. The bold values are significant at 95% confidence interval.

3.1.4 Atlantic Warm Pool Correlations

The Atlantic Warm Pool is the Atlantic component of the Western Hemisphere Warm Pool and can be defined as the area enclosed by a critical value (28.5°C) isotherm in the tropical Atlantic Ocean. This critical value is used because it displays the strongest interannual variations (Misra et. al., 2014). The onset and demise of the Atlantic Warm Pool can be defined in the same manner used in this study. The onset/demise of the Atlantic Warm Pool is defined as the day when the daily cumulative anomaly of the Atlantic Warm Pool area, west of 50°W and north of the equator, is at its minimum/maximum, respectively (Misra et. al., 2014). Considering the proximity to the study region, it is logical to evaluate the correlations between the Atlantic Warm Pool onset date, demise date, and area to the rainy season over Central America. In their paper, Misra et. al., 2014 find that years with a large Atlantic Warm Pool area are associated with excess seasonal rainfall over Central America during the August, September, and October months (Misra et. al., 2014). Table 4 shows the correlations between the Atlantic Warm Pool area, onset date, and demise date with the onset date, demise date, seasonal length, and seasonal rain of the wet season for each country in Central America. The bold values are significant at the 95% confidence interval according to the t-test. Once again, there are not many significant correlations present. However, Costa Rica and Panama, the two southernmost countries in Central America, display

		AWPA	AWPO	AWPD
GTM	Od	-0.009	0.088	0.011
	Dd	0.190	0.211	0.297
	LoS	0.112	0.082	0.185
	SR	-0.125	-0.146	-0.274
BLZ	Od	0.062	-0.205	0.218
	Dd	0.033	0.304	0.296
	LoS	0.077	0.210	0.087
	SR	-0.214	0.308	-0.309
SLV	Od	-0.017	0.150	-0.091
	Dd	-0.213	0.593	-0.024
	LoS	-0.096	0.188	0.023
	SR	-0.390	-0.122	-0.317
HND	Od	-0.262	0.006	-0.139
	Dd	-0.218	0.319	-0.213
	LoS	0.033	0.205	-0.058
	SR	-0.154	-0.044	-0.360
NIC	Od	-0.023	0.155	-0.043
	Dd	-0.066	0.005	-0.048
	LoS	-0.032	-0.110	-0.021
	SR	-0.410	0.089	**-0.479**
CRI	Od	0.200	0.294	0.150
	Dd	-0.296	-0.156	-0.360
	LoS	-0.274	-0.264	-0.302
	SR	**-0.509**	-0.099	**-0.466**
Pan	Od	0.145	0.400	0.009
	Dd	-0.230	-0.237	-0.175
	LoS	-0.203	-0.335	-0.113
	SR	**-0.467**	-0.127	-0.350

Table 4: The correlation of the area, onset date, and demise date of the Atlantic Warm Pool for a) Guatemala (GTM), b) Belize (BLZ), c) El Salvador (SLV), d) Honduras (HND), e) Nicaragua (NIC), f) Costa Rica (CRI), and g) Panama (PAN). with Onset date (Od), Demise date (Dd), Length of the Season (LoS), and Seasonal Rain (SR). The bold values are significant at 95% confidence interval.

consistent correlation signs. The onset date has a weak positive correlation between the Atlantic Warm Pool area, onset date, and demise date. The seasonal length and seasonal rain of the wet season in Costa Rica and Panama share a negative correlation between the Atlantic warm pool area, onset date, and demise date. In particular, there is a strong negative correlation between the seasonal rain in Costa Rica and Panama with the Atlantic Warm Pool area and the Atlantic Warm Pool demise.

3.1.5 Eastern Pacific Warm Pool Correlations

The Eastern Pacific Warm Pool is part of the larger Western Hemisphere warm pool. This warm pool can, similarly to the Atlantic Warm Pool, be defined as the region enclosed by the 28.5°C isotherm (Misra et. al., 2016). Also similar to the Atlantic Warm Pool, the Eastern Pacific Warm Pool lies right next to Central America and therefore could have a significant influence on the rainy season. The onset/demise of the Eastern Pacific Warm Pool is defined as the day when the daily cumulative anomaly of the Eastern Pacific Warm Pool area, west of 50°W and north of the equator, is at its minimum/maximum, respectively (Misra el. al., 2016). Table 5 shows the correlations between the Eastern Pacific Warm Pool area, onset date, and demise date with the onset date, demise date, seasonal length, and seasonal rain of the wet season for each country in Central America. The bold values are significant at the 95% confidence interval according to the t-test. Again, there are not many significant correlations present in the table with the correlations in the northernmost countries in Central America harboring the higher correlations. There are significant correlations between the Eastern Pacific Warm Pool area with the demise date of the wet season over Honduras. There are no significant correlations between the Eastern Pacific Warm Pool onset date and any of the rainy season variables for any of the countries in South America. The Eastern Pacific Warm Pool demise date does exhibit a positive correlation with the demise date of the wet season over Guatemala. However, more promising is the shared negative correlations between the Eastern Pacific Warm Pool demise dates with the seasonal rain shown for all countries. This indicates an earlier Eastern Pacific Warm Pool demise is correlated to a later Central America rainy season demise date. However, only Guatemala and El Salvador show a significant negative correlation.

		EPWPA	EPWPO	EPWPD
GTM	Od	-0.102	0.137	0.064
	Dd	-0.118	-0.019	**0.473**
	LoS	-0.006	-0.085	0.238
	SR	-0.012	0.080	**-0.434**
BLZ	Od	0.080	-0.098	0.119
	Dd	-0.186	-0.274	0.247
	LoS	-0.038	-0.207	0.037
	SR	-0.087	0.335	-0.178
SLV	Od	-0.067	0.002	0.144
	Dd	-0.381	0.169	0.282
	LoS	-0.160	0.084	0.037
	SR	-0.226	0.069	**-0.492**
HND	Od	-0.259	-0.159	0.029
	Dd	**-0.440**	0.195	0.168
	LoS	-0.123	0.258	0.084
	SR	-0.092	0.313	-0.404
NIC	Od	-0.338	0.020	-0.090
	Dd	-0.175	-0.192	-0.111
	LoS	0.091	-0.152	-0.014
	SR	-0.157	0.027	-0.334
CRI	Od	-0.075	0.012	0.205
	Dd	-0.052	-0.023	-0.158
	LoS	0.003	-0.046	-0.211
	SR	-0.054	0.011	-0.346
Pan	Od	-0.114	0.336	0.069
	Dd	0.133	-0.196	0.015
	LoS	0.130	-0.281	-0.050
	SR	-0.111	-0.078	-0.192

Table 5: The correlation of the area, onset date, and demise date of the Eastern Pacific Warm Pool for a) Guatemala (GTM), b) Belize (BLZ), c) El Salvador (SLV), d) Honduras (HND), e) Nicaragua (NIC), f) Costa Rica (CRI), and g) Panama (PAN). with Onset date (Od), Demise date (Dd), Length of the Season (LoS), and Seasonal Rain (SR). The bold values are significant at 95% confidence interval.

3.1.6 Probabilistic Skill of Seasonal Outlook

Using the methodology described in Section 2.2.4, four ROC curves for each country in Central America were developed to quantify the predictability potential of the onset date on the seasonal length and seasonal rain. The expectation, following the correlations shown in Table 2, is that an early onset date should correspond with a longer and wetter season, and a late onset date should correspond with a shorter and dryer season. These categorical seasonal outlooks

based on the variations of the onset date of the rainy season are evaluated by the AROC metric displayed in Figure 8. With the only exception being the correspondence of a late onset date leading to a dryer season in Guatemala, all other AROC values for all the other countries are above 0.5, suggesting a reliable seasonal outlook can be obtained from monitoring the onset of the rainy season. In general, using the onset date to predict if the season will be longer or shorter than normal shows more skill than using the onset date to predict if the season will be wetter or dryer than normal.

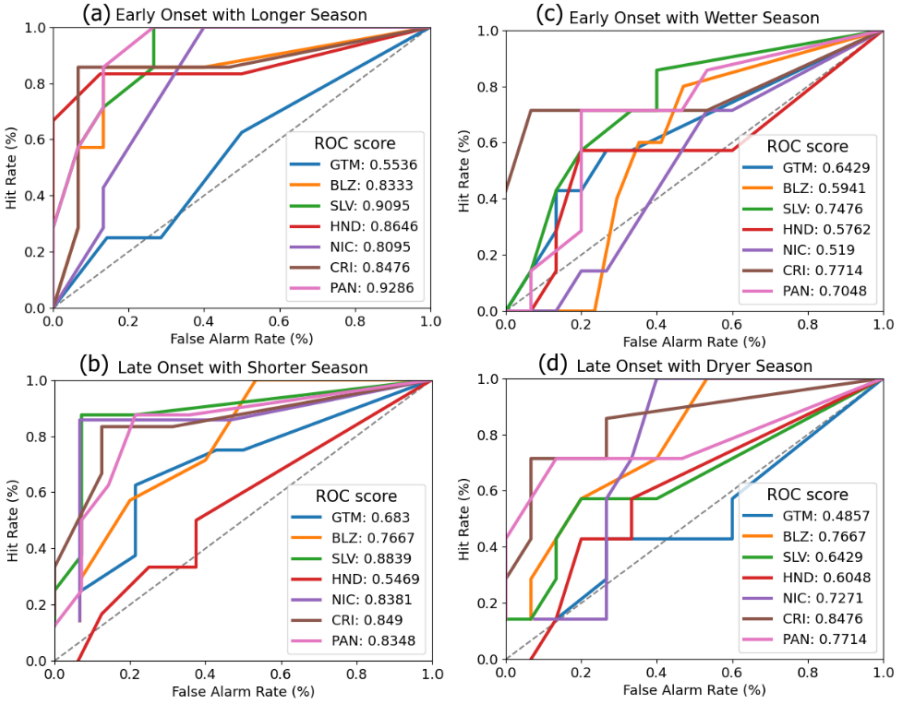

Figure 8: The area under the relative operating characteristic curve of the outlook for (a, b) seasonal length and (c,d) seasonal rain based on onset date variations for Guatemala (GTM), Belize (BLZ), El Salvador (SLV), Honduras (HND), Nicaragua (NIC), Costa Rica (CRI), and Panama (PAN).

3.2 Local Diagnosis

The area-averaged precipitation over the seven countries provides a quick and easy look at the evolution of the rainy season. However, given the complex geography of the region, it is safe to expect significant spatial heterogeneity in the evolution of the rainy season over Central America, which is not captured in the area-averaged analysis of the previous section. In this

section, the results of the analysis conducted at the spatial resolution of IMERG (~10km grid) are discussed.

3.2.1 Climatology

Figures 9a-d show the climatology of the onset, demise, length, and seasonal rainfall of the wet season. Since an ensemble of 1001 members is generated from the methodology, the median value of the diagnosed onset, demise, length, and seasonal rain for each wet season is used to compute this climatology to avoid the influence of outliers. Figure 9a shows that the onset date is generally earlier on the Pacific coast than on the Atlantic coast. Furthermore, the earliest onset dates appear in Panama, and onset dates gradually occur later in the year proceeding farther north. However, this progression is not uniform with parts of the Pacific coast of Costa Rica, Nicaragua, and El Salvador displaying later onset dates compared to parts of Honduras and Guatemala. The west-to-east progression of the onset date of the wet season is, however, more uniform across Central America (Figure 9a).

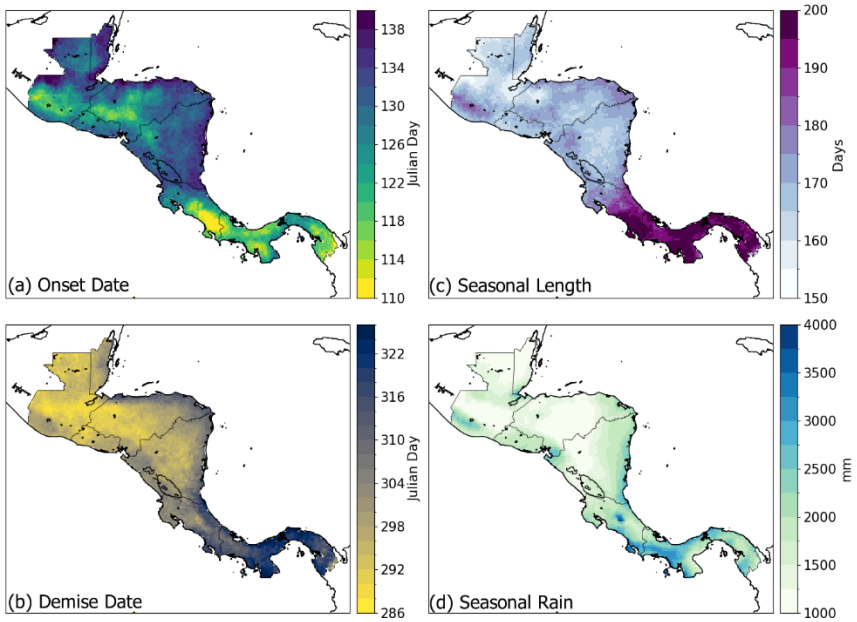

Figure 9: The 22-year (2001-2022) climatological median (a) onset date (Julian Day), (b) demise date (Julian Day), (c) seasonal length (days), and (d) seasonal rain from 12h latency IMERG product.

Similarly, the demise date shows a meridional and a zonal gradient in Figure 9b. For example, the later demise dates in Panama and Costa Rica to the rest of Central America are apparent. Furthermore, the Atlantic coast of Central America displays a later demise date than the Pacific coast, with areas between the coasts in Nicaragua, Honduras, and Guatemala showing some of the earliest demise dates of the wet season (Figure 9b).

Consequently, the length of the wet season is the longest in Panama and parts of Costa Rica from a relatively earlier and a later onset and demise date of the wet season, respectively (Figure 9c). Climatologically, some of the shortest wet season is in Belize and the interiors of Guatemala, Honduras, and Nicaragua (Figure 9c). It is this spatial variation of the length of the season that is often missed when wet seasons are fixed to calendar months across Central America.

The corresponding climatological seasonal mean rainfall accumulated from the day of the onset to the day of the demise of the wet season is shown in Figure 9d. Generally, longer seasons correspond to higher seasonal rain in Panama and Costa Rica. However, the correspondence between the length of the season (Figure 9c) and the seasonal rain (Figure 9d) is not so obvious with parts of Panama and Costa Rica displaying far less seasonal rain and is comparable to other northern parts of Central America despite its comparatively longer length of the wet season. This implies that the daily rain rates in the wet season are relatively weaker in some of these regions in Panama and Costa Rica. Belize and the interiors of Nicaragua, Honduras, and Guatemala receive some of the lowest seasonal rain in the wet season compared to other parts of Central America.

Comparing these onset dates and demise dates to Gramzow and Henry (1972) reveals many similarities. Though the dates differ, the spatial patterns of the evolution of the rainy season are rather analogous. The earliest dates in both Gramzow and Henry (1972) (Figure 2) and in this study (Figure 9a) occur in Costa Rica and Panama. However, the results in Figure 2 display the start of the season on the Caribbean side of Central America whereas such a start is not evident in this study. The latest onset dates are long in the Northern countries, hugging the Caribbean coastline (Figure 9a). This is shown for Honduras in Figure 2, but not Nicaragua as seen in Figure 9a. The sliver of early onsets in El Salvador is apparent in both Figure 2 and Figure 9a. Finally, the late onset dates shown in Figure 2 above Lake Nicaragua are not seen in Figure 9a. The spatial evolution of the demise dates is even more similar with the largest difference being the dates (Figure 3 and Figure 9b). Though there are obvious differences in the datasets used and methodology between this study and that of Gramzow and Henry (1972), the similarities of both should be acknowledged.

3.2.2 Onset, Demise, Seasonal Length, and Seasonal Rain Correlations

The four variables shown in Figure 9 display considerable variability as noted by their standard deviation (Figure 10). Furthermore, the standard deviation exhibits strong spatial gradients in the variations of the onset date, demise date, length, and seasonal rain of the wet season (Figure 10). Therefore, understanding the variations in the length of the season and their implication on the seasonal rain of the wet season on local or small spatial scales is important.

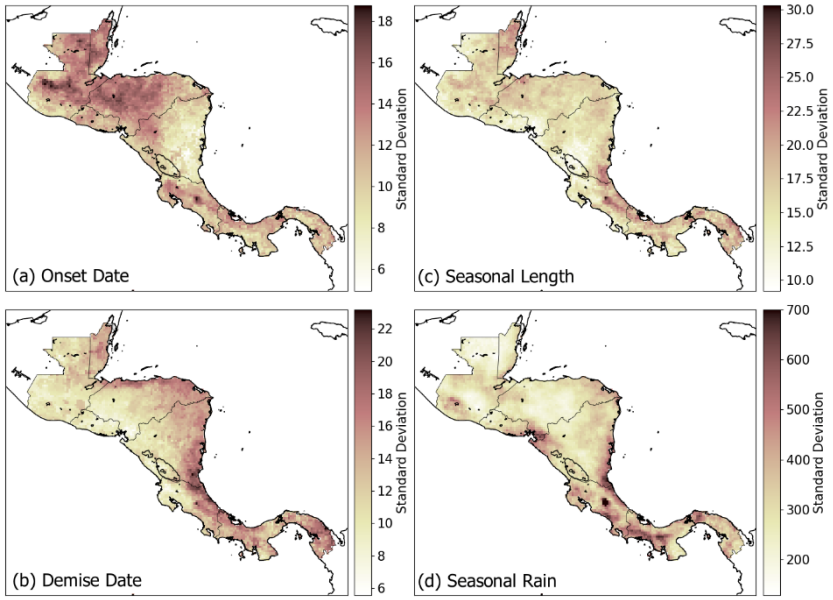

Figure 10: The standard deviation of (a) onset date (days), (b) demise date (days), (c) length (days), and (d) seasonal rain (mm) of the wet season.

In Figure 11c, the correlations of the median onset date (diagnosed from the 1001 ensemble members) with the corresponding median seasonal length of the wet season are shown. The correlations are significantly large and negative except near the Atlantic coast of Nicaragua and Honduras (Figure 11c). The negative correlations in Figure 11c suggest that an early or a later onset date of the wet season is associated with a longer or shorter wet season, respectively. Furthermore, in Figure 11b the correlations of the onset date with the corresponding seasonal rainfall anomaly of the wet season are shown, which yet again highlights the importance of the onset date variations. The regions of Central America that exhibit statistically significant correlations in Figure 11b suggest that an early or a later onset is associated with a wetter or drier wet season, respectively. However, the statistically significant correlations between the onset and the demise dates are isolated and rare (Figure 11a). This implies that the influence of the onset date variations on the length and the seasonal rain of the wet season is relatively independent of the influence of the demise date variations. In summary, Figure 11b-c suggests that monitoring the onset date of the wet season has the benefit of providing an outlook of the forthcoming length

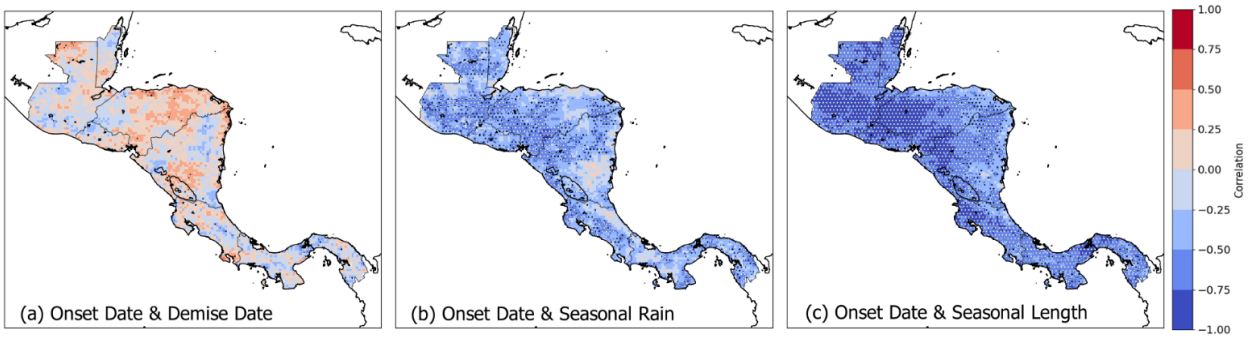

Figure 11: The correlations of the onset date with anomalies of (a) demise date (b) length, and (c) seasonal rain. The statistically significant values at a 5% significance level according to the t-test are stippled black. The statistically significant values at a 1% significance level according to the t-test are stipple white.

and seasonal rainfall anomaly of the wet season over most of Central America. Likewise, the positive correlations of demise date with seasonal rain over Panama, Costa Rica, parts of the Atlantic coast of Nicaragua and Honduras, and Belize suggest that early or later demise is associated with drier or wetter wet seasons, respectively (Figure 12a). It is apparent comparing Figures 12a and 11b, that the regions of overlap with significant correlations are relatively small. For example, the correlations in Figure 11b over interior Honduras, Guatemala, and the west coast of Nicaragua are strong while it is weak in Figure 12a, suggesting that variations in onset and demise date complement each other in associating with corresponding changes in the seasonal rainfall. However, unlike onset date variations which offer the luxury to foretell the evolution of the forthcoming wet season the demise date variations can only posteriorly explain the seasonal rainfall anomalies of the wet season.

Similarly, the correlations of the demise date variations with the corresponding anomalies of the length of the wet season are shown in Figure 12b. In comparing Figure 12b with Figure 11c, there is significant overlap in the regions where demise and onset date variations affect the seasonal length. However, more subtly, in some of the regions along the Atlantic coasts of Nicaragua and Honduras, the demise date variations have a significant correlation with the length of the wet season (Figure 12b) compared to the insignificant correlations between the onset date and length of the wet season in Figure 11c. In contrast, the correlations between the onset date and the seasonal length are relatively significant in western Honduras (Figure 11c) while the correlations between the demise date and length of the season are weak (Figure 12b).

However, given that in many of these regions the co-variability between onset and demise dates is weak (Figure 11a), their corresponding influence on the seasonal length and seasonal rain are independent of each other. The statistically significant positive correlations in Figure 12b suggest that early or later demise of the wet season is associated with shorter or longer length of the wet season, respectively.

The seasonal length anomalies have a widespread and significant relationship with seasonal rain of the wet season across Central America (Figure 12c). There are some exceptions where the length of the season variation does not covary significantly with seasonal rain (Figure 12c). For example, in the region bordering Costa Rica and Nicaragua, parts of the Atlantic coasts of Nicaragua and Honduras, and some parts of Guatemala where neither the onset date (Figure 11b) nor the demise date (Figure 12a) variations have a significant influence on the seasonal rain.

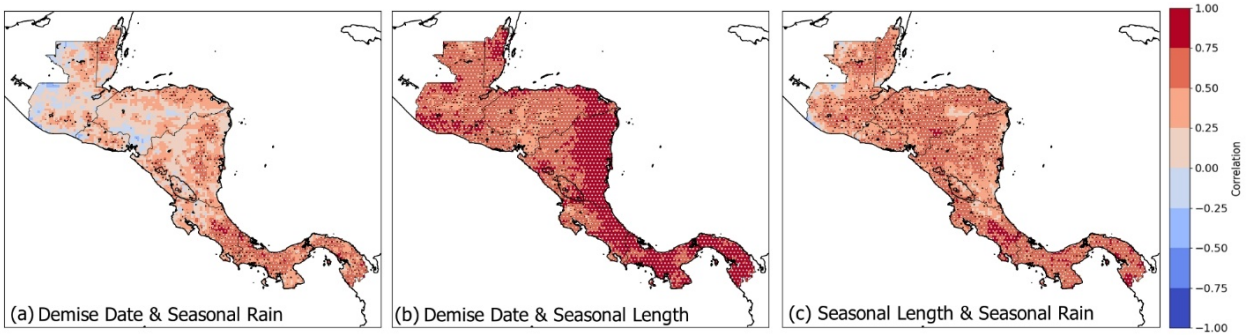

Figure 12: The correlations of the demise date with anomalies of (a) seasonal rain and (b) seasonal length of the wet season. (c) The correlations of the seasonal length with corresponding seasonal rainfall anomalies of the wet season. The statistically significant values at a 5% significance level according to the t-test are stippled black. The statistically significant values at a 1% significance level according to the t-test are stipple white.

3.2.3 ENSO Correlations

The correlations in Figures 11b and c and Figures 12a and b assume significance in the fact that other potential external forcings like the ENSO variability, the Eastern Pacific Warm Pool, and the Atlantic Warm Pool variations have comparatively far less bearing on the seasonal variations of the wet season of Central America. In other words, the correlations in Figures 11 and 12 reflect the local relationships that dictate the seasonal evolution of the wet season over Central America, which are not necessarily dictated by large-scale climate variations.

Figure 13 displays the correlations between the DJF (-1) Niño 3.4 SST index with onset date, demise date, seasonal length, and seasonal rain. There are very few significant correlation values plotted with the highest significance over Lake Nicaragua shown for the onset date and seasonal length (Figures 13a and 13c). Interestingly, the maps of the correlations for seasonal length and demise are remarkably similar spatially. Further, the map of the onset date is similar as well, though opposite in magnitude. This is likely due to the correlations shown in Figures 11c and 12b where the onset date and the seasonal length have a negative correlation and the demise date and the seasonal length have a positive correlation. The correlations plotted in Figure 13d are small but generally negative.

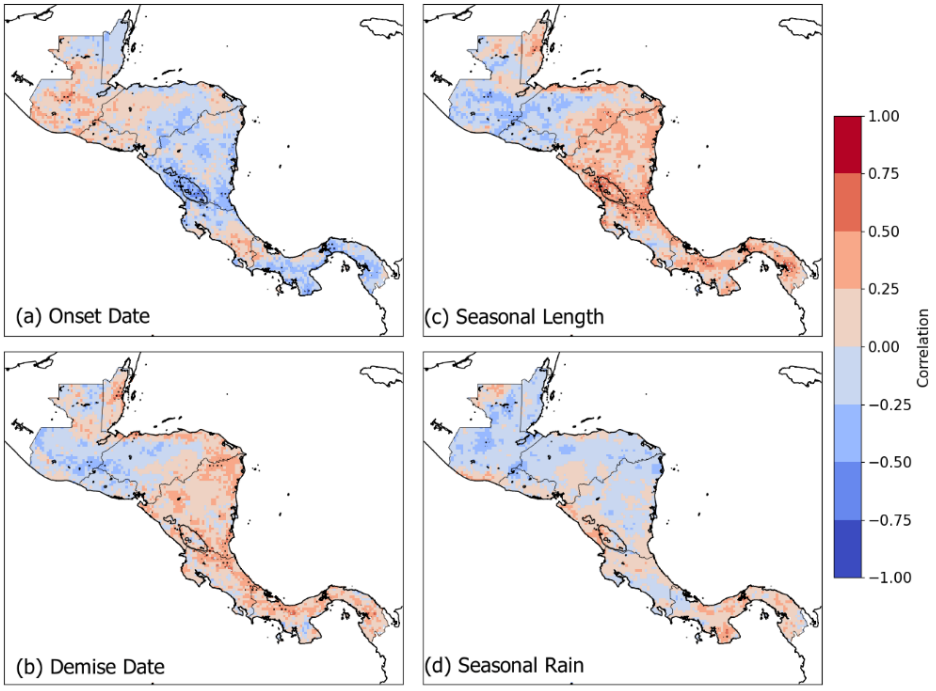

Figure 13: The correlations of the DJF (-1) Nino3.4 SST index (OISSTv2; Reynolds et al. 2002) with anomalies of (a) onset date, (b) demise date, (c) seasonal length, and (d) seasonal rain of the rainy season. The statistically significant values at a 5% significance level according to the t-test are stippled black. The statistically significant values at a 1% significance level according to the t-test are stippled white.

Figure 14 displays the correlations between the MAM Niño 3.4 SST index with onset date, demise date, seasonal length, and seasonal rain. These correlations are very similar in both magnitude and spatial distribution as in Figure 13 with the exception of Figure 14d. Again, the

correlations between the onset and seasonal length and the demise and seasonal length are apparent (Figures 114a-c). The correlations between MAM Niño 3.4 SST index with seasonal rain as shown in Figure 14d are much more uniformly negative with higher values of correlation than shown in Figure 13d.

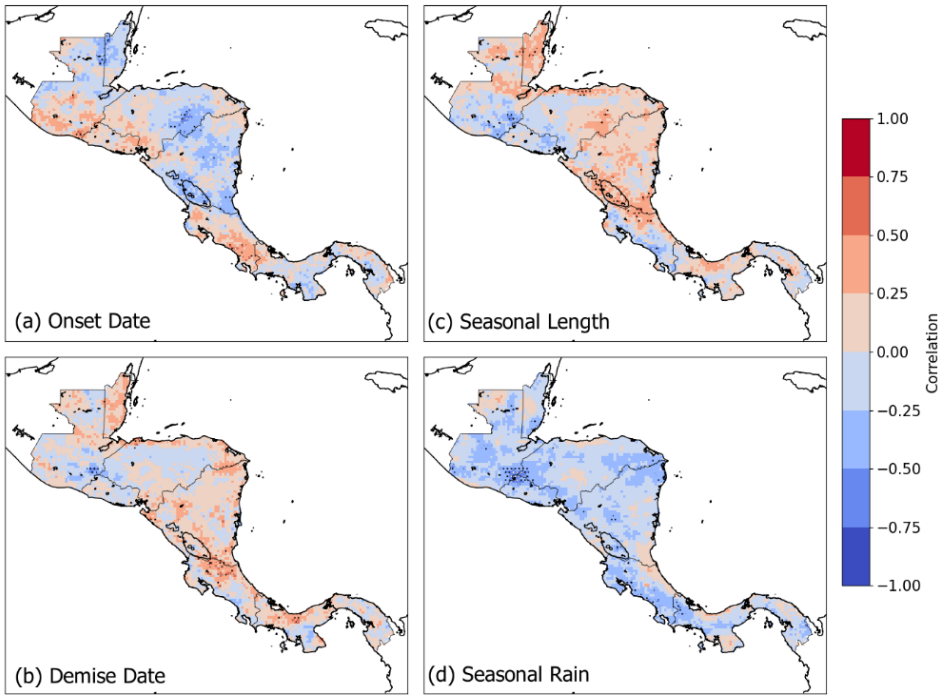

Figure 14: The correlations of the MAM Nino3.4 SST index (OISSTv2; Reynolds et al. 2002) with anomalies of (a) onset date, (b) demise date, (c) seasonal length, and (d) seasonal rain of the rainy season. The statistically significant values at a 5% significance level according to the t-test are stippled black. The statistically significant values at a 1% significance level according to the t-test are stippled white.

Figure 15 displays the correlations between the JJA Niño 3.4 SST index with onset date, demise date, seasonal length, and seasonal rain. The correlations between the JJA Niño 3.4 SST index with onset date are insignificant for most of Central America (Figure 15a). However, there is a pattern of significant positive correlations along the west coast, primarily in Nicaragua, with opposing negative correlations along the east coast. The correlations between the JJA Niño 3.4 SST index and with demise date do not display any clear patterns and have very few significant values (Figure 15b). The seasonal length correlations (Figure 15c) are generally the same as the

demise date correlations and opposite of the onset date correlations (Figure 15a). Again, recalling the correlations between onset date and seasonal length and demise date and seasonal length displayed in Figures 11c and 12b, it is likely the agreement shown between Figures 15c and d and the reversal shown between Figures 15a and c is a consequence of this relationship. The correlations between JJA Niño 3.4 SST index with seasonal rain are overwhelmingly negative with many values significant at the 1% significance level according to the t-test (Figure 15d). These correlations appear to be an intensification of the correlations shown in Figures 13d and 14d. The significant values are mainly clustered on the North and West sides of Central America.

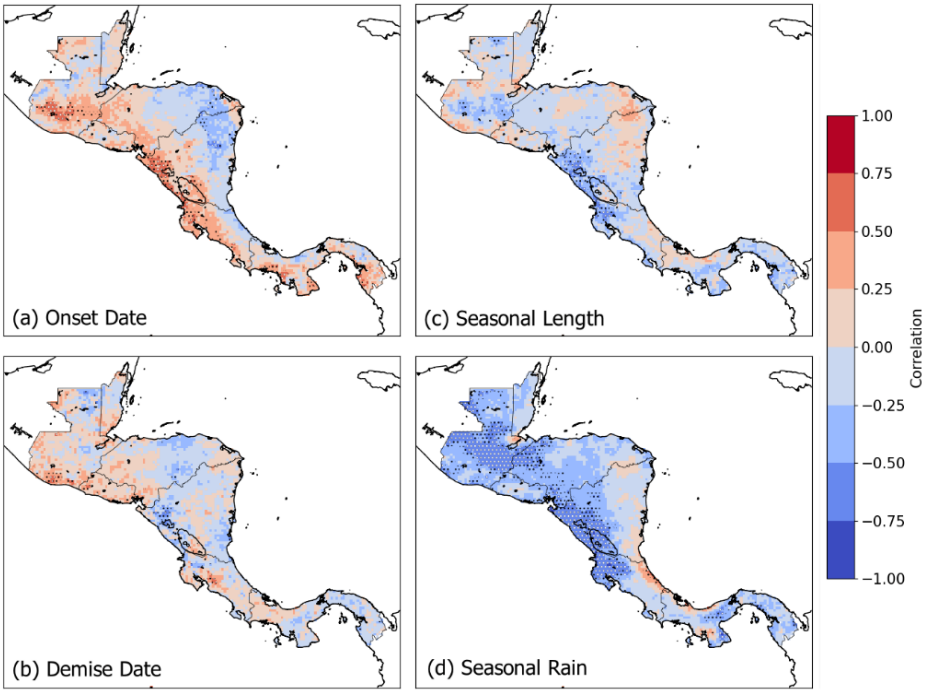

Figure 15: The correlations of the JJA Nino3.4 SST index (OISSTv2; Reynolds et al. 2002) with anomalies of (a) onset date, (b) demise date, (c) seasonal length, and (d) seasonal rain of the rainy season. The statistically significant values at a 5% significance level according to the t-test are stippled black. The statistically significant values at a 1% significance level according to the t-test are stippled white.

3.2.4 Atlantic Warm Pool Correlations

To examine the potential connections between the Atlantic Warm Pool with the Central American rainy season, correlation maps were created. Figure 16 shows the correlations between the Atlantic Warm Pool onset date with the onset date, demise date, seasonal length, and seasonal rain for the rainy season over Central America. Figure 16a shows mostly insignificant positive correlations with the exception of statistically significant values at a 1% level according to the t-test present over western Nicaragua. Figure 16b displays very weak and scattered correlations. As seen previously with the ENSO correlations, the onset date correlations and seasonal length correlations are loosely reversed, and the demise date and seasonal length share similar spatial patterns as seen in Figures 13 and 14, though it is less apparent in Figure 16.

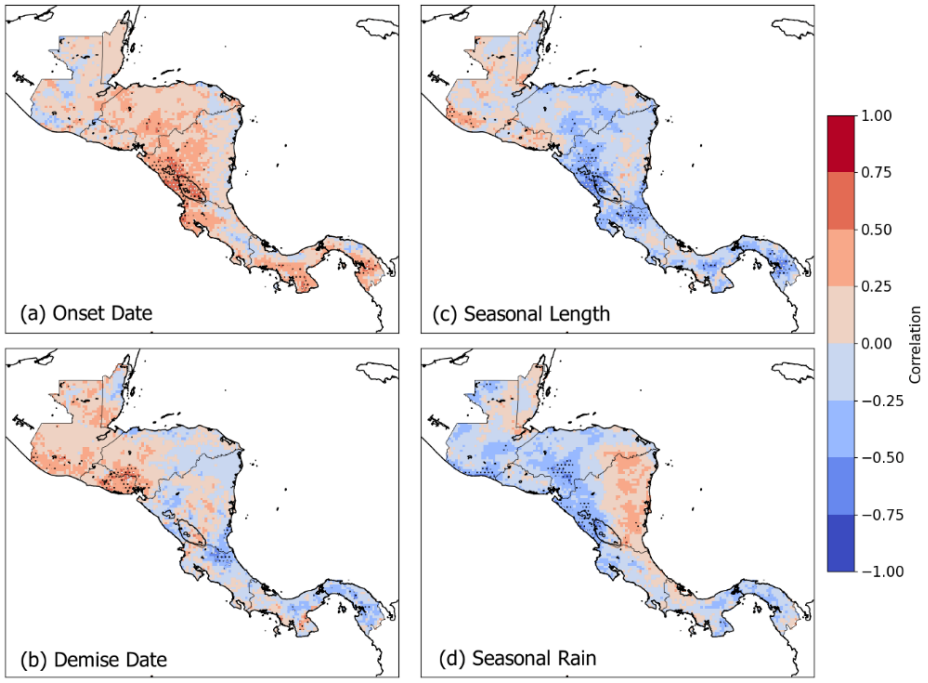

Figure 16: The correlations of the Atlantic Warm Pool onset date (Misra et al. 2014; OISSTv2; Reynolds et al. 2002) anomalies of (a) onset date, (b) demise date, (c) seasonal length, and (d) seasonal rain of the rainy season. The statistically significant values at a 5% significance level according to the t-test are stippled black. The statistically significant values at a 1% significance level according to the t-test are stippled white.

Figure 16d displays weak correlations between the Atlantic Warm Pool onset and the seasonal rain over Central America; however, there is a distinct pattern of positive correlations along the eastern side of Central America and negative correlations along the western side. This is mainly observed in the central section of Central America running from Nicaragua through parts of Panama.

Similarly, Figure 17 shows the correlations between the Atlantic Warm Pool demise date with the onset date, demise date, seasonal length, and seasonal rain for the rainy season over Central America. Again, the correlations are weak and scattered. The patterns between the relationships between the onset date, demise date, and seasonal length are again present in Figures 17a-c. Notably, there are some grouped statistically significant values present along the eastern side of Central America Figure 17d. This region is shared with the correlations shown in Figure 16d, though in Figure 17d, they are stronger and opposite those in Figure 16d.

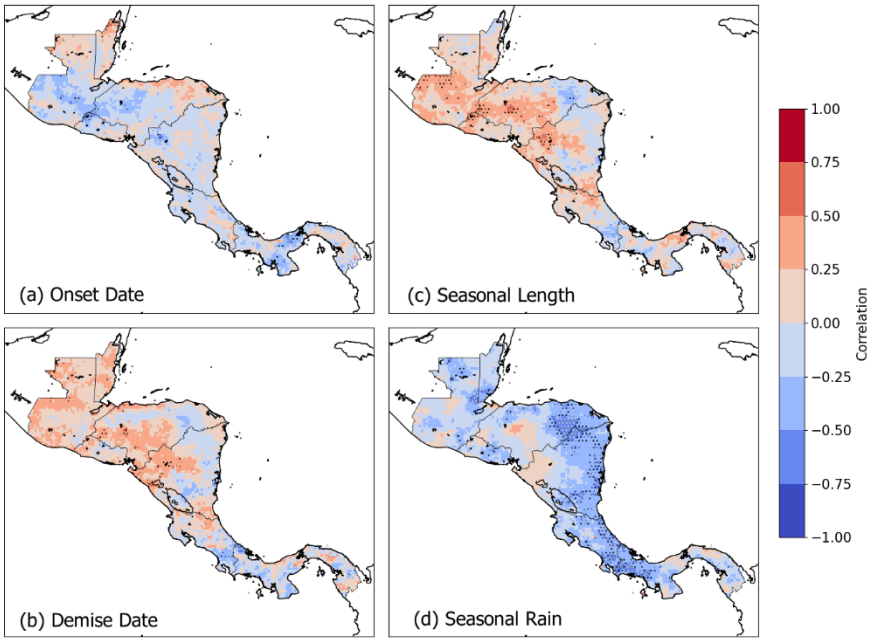

Figure 17: The correlations of the Atlantic Warm Pool demise date (Misra et al. 2014; OISSTv2; Reynolds et al. 2002) anomalies of (a) onset date, (b) demise date, (c) seasonal length, and (d) seasonal rain of the rainy season. The statistically significant values at a 5% significance level according to the t-test are stippled black. The statistically significant values at a 1% significance level according to the t-test are stippled white.

Figure 18, again, does not show very promising correlations. The correlations between the Atlantic Warm Pool area with the onset date and demise date of the Central American rainy season are largely insignificant (Figures 18a-b). There are some statistically significant values for the correlation between the Atlantic Warm Pool area and the seasonal length and seasonal rain (Figures 18c-d). For the seasonal length correlation map (Figure 18c), there is a region of positive correlations clustered along the west coast of Nicaragua that extends through the center

of Honduras. The seasonal rain correlation map (Figure 18d) displays statistically significant values at a 1% significant level according to the t-test from parts of western Panama through southern Costa Rica. Again, it is interesting to see the consistent patterns seen through the onset date, demise date, and seasonal length correlation plots as mentioned in previous Figures (Figures 18a-c).

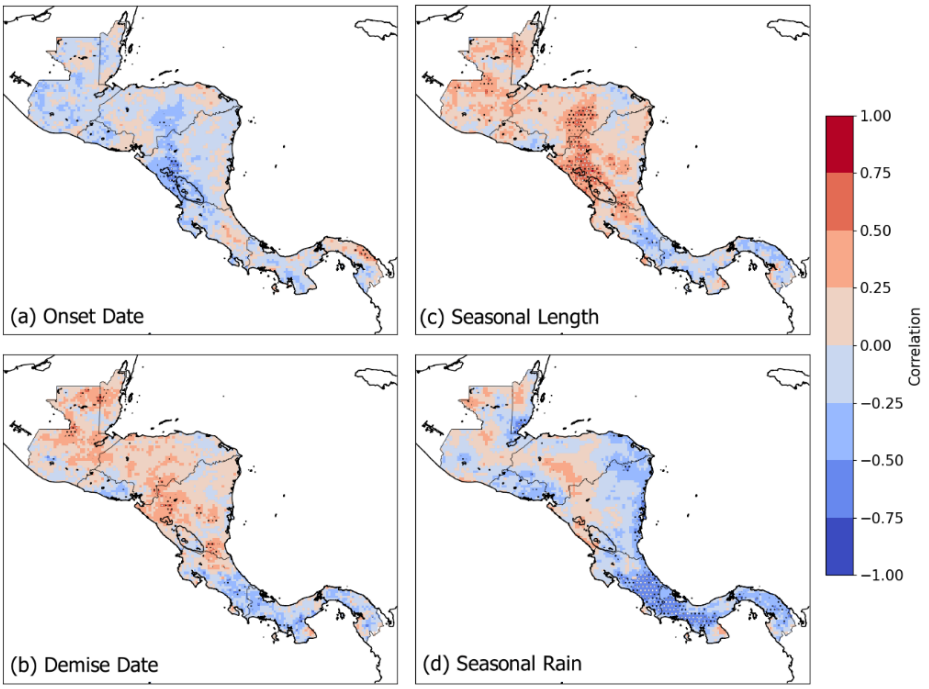

Figure 18: The correlations of the Atlantic Warm Pool area (Misra et al. 2014; OISSTv2; Reynolds et al. 2002) anomalies of (a) onset date, (b) demise date, (c) seasonal length, and (d) seasonal rain of the rainy season. The statistically significant values at a 5% significance level according to the t-test are stippled black. The statistically significant values at a 1% significance level according to the t-test are stippled white.

3.2.5 Eastern Pacific Warm Pool Correlations

The Atlantic Warm Pool shows little promise in explaining or helping to forecast the spatial patterns of the onset date, demise date, seasonal length, and seasonal rain of the rainy season over Central America. The Eastern Pacific Warm Pool correlation maps are about equal in their significance to the Atlantic Warm Pool correlation maps. Figure 19 displays the maps of the Eastern Pacific Warm Pool onset correlations with the onset date, demise date, seasonal

length, and seasonal rain of the Central America rainy season. Correlations displayed are mainly insignificant with the exception of the border between Nicaragua and Costa Rica where there are negative correlations between the Eastern Pacific Warm Pool onset and the demise date and seasonal length of the Central America rainy season significant at 5% and few at the 1% significance level according to the t-test for the (Figures 19b-c).

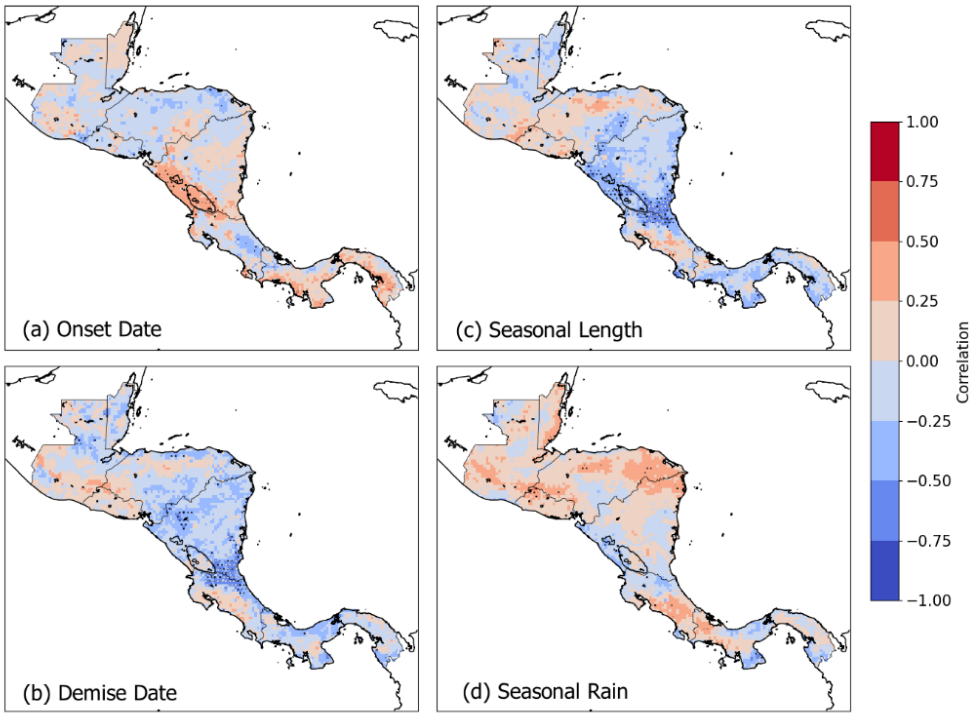

Figure 19: The correlations of the Eastern Pacific Warm Pool onset date (Misra et al. 2016; OISSTv2; Reynolds et al. 2002) with anomalies of (a) onset date, (b) demise date, (c) seasonal length, and (d) seasonal rain of the rainy season. The statistically significant values at a 5% significance level according to the t-test are stippled black. The statistically significant values at a 1% significance level according to the t-test are stippled white.

Figure 20 displays the maps of the Eastern Pacific Warm Pool demise correlations with the onset date, demise date, seasonal length, and seasonal rain of the Central America rainy season. There are few significant correlations with little spatial agreement for Figures 20a and c. Figure 20b does display some continuity in the spatial arrangement of the correlations and significant regions. The northern regions of Central America are dominated by positive

correlations whereas the southern region is more negative (Figure 20b). However, the most significant are the correlations between the Eastern Pacific Warm Pool demise date with the seasonal rain over Central America shown in Figure 20d. The vast majority of Central America displays negative correlations with clusters of significant values along the western coasts (Figure 20d). Unfortunately, these correlations are unlikely to assist a forecast because the demise dates of the Eastern Pacific Warm Pool tend to occur very late in the Central American rainy season.

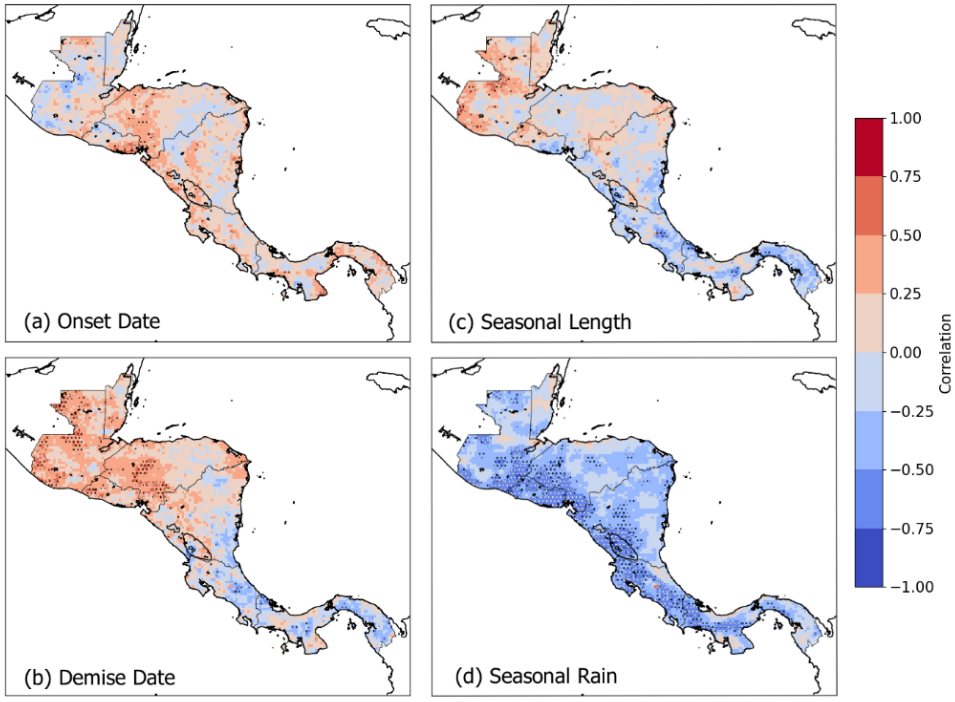

Figure 20: The correlations of the Eastern Pacific Warm Pool demise date (Misra et al. 2016; OISSTv2; Reynolds et al. 2002) with anomalies of (a) onset date, (b) demise date, (c) seasonal length, and (d) seasonal rain of the rainy season. The statistically significant values at a 5% significance level according to the t-test are stippled black. The statistically significant values at a 1% significance level according to the t-test are stippled white.

Figure 21 displays the maps of the Eastern Pacific Warm Pool area correlations with the onset date, demise date, seasonal length, and seasonal rain of the Central America rainy season. Figures 21b-d show overwhelmingly insignificant correlation values with little spatial agreement. Figure 21a displays a region of consistently negative values with few statistically significant grids through central Nicaragua into Honduras.

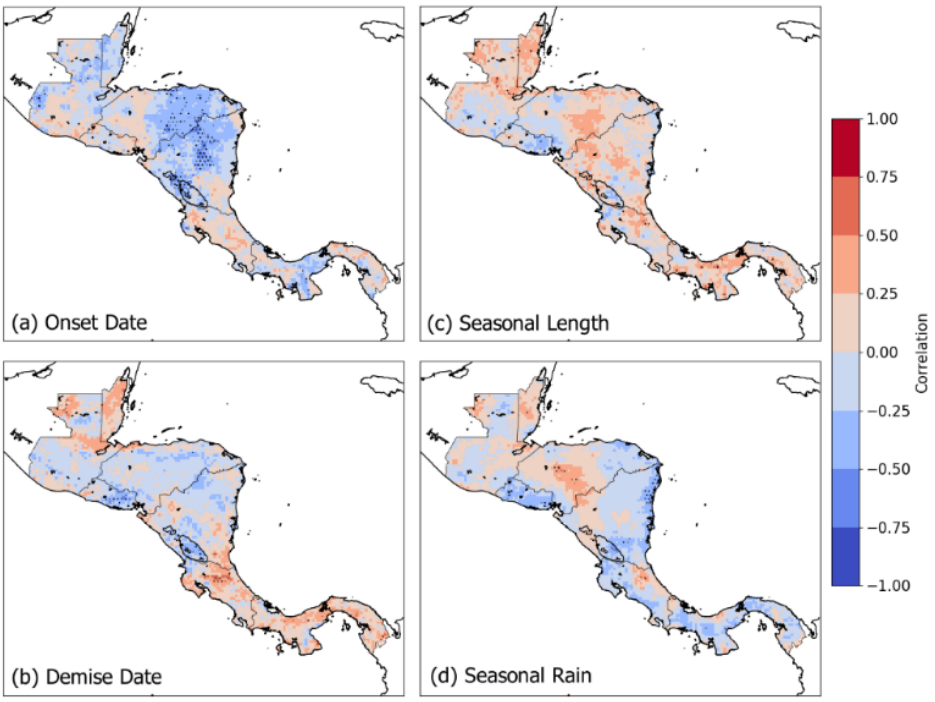

Figure 21: The correlations of the Eastern Pacific Warm Pool area index (Misra et al. 2016; OISSTv2; Reynolds et al. 2002) with anomalies of (a) onset date, (b) demise date, (c) seasonal length, and (d) seasonal rain of the rainy season. The statistically significant values at a 5% significance level according to the t-test are stippled black. The statistically significant values at a 1% significance level according to the t-test are stippled white.

3.2.6 Probabilistic Skill of Seasonal Outlook

Given the comparatively weak external forcing of large-scale climate variability on the wet season variations of Central America (Figures 13-21), the relationship between the onset date and the seasonal length and seasonal rain could be exploited for real-time monitoring and outlook of the evolution of the forthcoming wet season. Figure 22 shows maps of the AROC score for the outlook of seasonal length and seasonal rainfall anomalies based on anomalous early and late-onset seasons. The AROC measures the probabilistic skill of the outlook, which is obtained from the 1001-member ensemble of the adopted methodology. The outlook at a given grid point in the domain is considered useful if its corresponding AROC curve is ≥ 0.5 (Narotsky and Misra 2021). The anomalous onset dates, length of the season, and seasonal rain

are considered when they are not in the middle but extreme terciles. In Figure 22a, the outlook of a long wet season from early onset has a very high AROC, well over 0.5 across Central America, with rare exceptions in pockets over Costa Rica and along the Atlantic coasts of Nicaragua and Honduras. Similarly, the outlook of the short wet season from the late onset is also promising (Figure 22c). There are however slightly more widespread regions of low skill scores (< 0.5 AROC) along the Atlantic coasts of Nicaragua and Honduras (Figure 22c) compared to outlook from early onset seasons (Figure 22a). In contrast, the skills along the northwestern part of Central America in Figure 22b are much higher and more widespread than in Figure 22a.

The outlook of the wetter season in early onset seasons also shows considerable probabilistic skill with widespread areas across Central America exhibiting AROC ≥ 0.5 (Figure 22cb. From Belize to Panama and in all the intervening countries in between, there are significant regions with an AROC ≥ 0.5 (Figure 22b). However, there are also larger pockets of regions with weaker to no probabilistic skill (Figure 22b) compared to the length of the season (Figure 22a). Similarly, the outlook of the drier wet season from the late onset of the season also shows widespread probabilistic skill across Central America (Figure 22d). In fact, the magnitude of the AROC curve in Figure 19d is slightly higher than in Figure 22c, suggesting that the likelihood of a drier season from the later onset of the season has a higher probability of validating than the likelihood of a wetter season from the earlier onset, especially over western Honduras, El Salvador, parts of Guatemala and Belize.

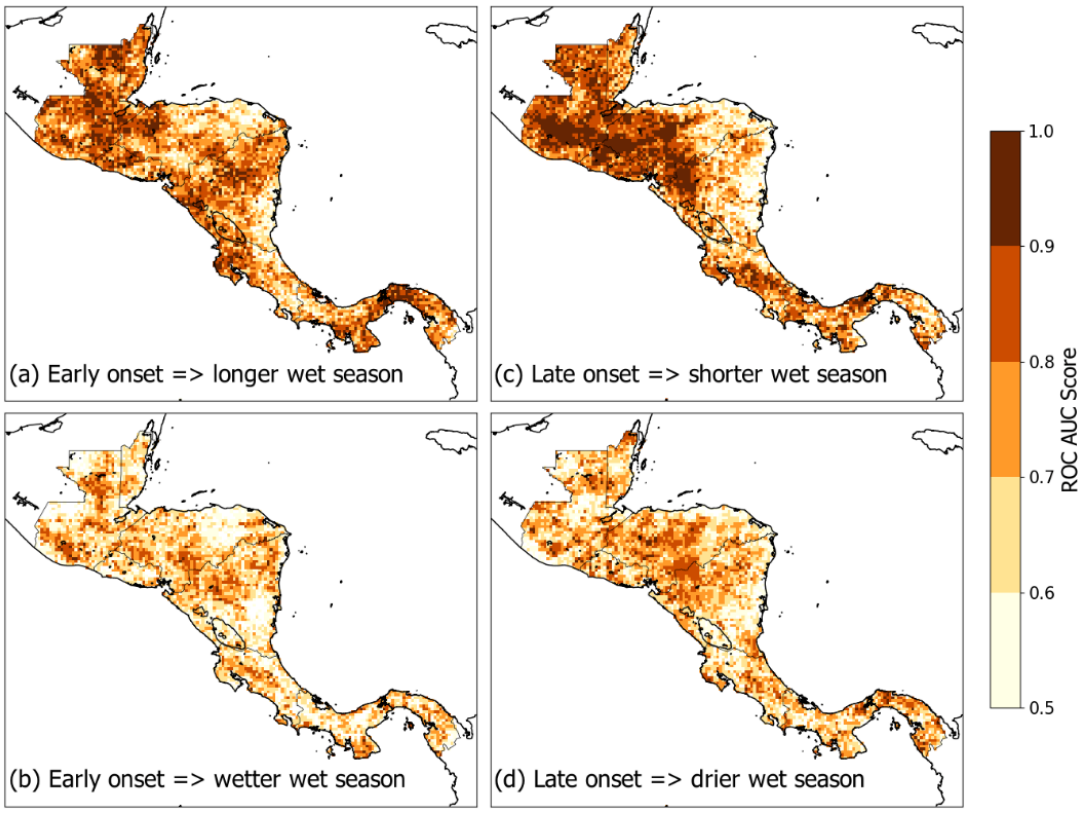

Figure 22: The area under the Relative Operating Characteristic (ROC) curve for the outlook of a) a longer wet season based on early onset, b) a wetter wet season based on early onset, c) a shorter wet season based on later onset, and d) drier wet season based on later onset of the wet season. Only regions with an area under the ROC curve ≥ 0.5, which signifies probabilistic skill that is better than random forecast are shaded.

CHAPTER 4

CONCLUSIONS

Central America, with its complex geography of an isthmus, steep orography, and diverse vegetation features offers a stiff challenge to predict its hydroclimate at all spatial and temporal scales. As shown earlier in this study, the influence of external forcings such as ENSO, the Eastern Pacific Warm Pool, and the Atlantic Warm Pool variations has a very modest bearing on the seasonal variations of the rainy season over Central America. A robust and objective way of defining the onset and the demise of the rainy season from observed daily time series of rainfall is introduced that can be applied on both a regional scale and a local scale. The proposed methodology includes the variations in the length of the season in accounting for the variability of the wet season that is otherwise ignored in the fixed calendar month definitions of the season.

4.1 Area Averaged Diagnosis

At a regional scale, the calculations are much faster, and the results are still meaningful. These results may be more influential to policymakers as the variables are solved based on political boundaries. There are very few significant correlations between the onset date, demise date, seasonal length, and seasonal rain with the Nino3.4 SST index. This is also true for the correlations with the Atlantic Warm Pool variables and the Eastern Pacific Warm Pool variables. However, there are many significant correlations between the onset date with the seasonal length and seasonal rainfall that may be exploited for forecasting purposes. The ROC curves (Figure 8) serve to emphasize this point. However, the coarse granularity of this area averaged analysis does not allow analysis of the spatial heterogeneity in the evolution of the rainy season over Central America. Given the complex geography of the region, the evolution of the rainy season has both zonal and meridional gradients, which is lost in area averaging over the countries.

4.2 Local Diagnosis

While there are benefits to applying the methodology on a regional scale, the intricate patterns of the evolution of the rainy season are lost. Instead, applying the methodology to the native resolution of the IMERG dataset recovers these important discrete patterns that are lost by relying on the political boundaries of the countries. At this local scale, the correlations between

the large-scale climate variables (e.g., ENSO index and western hemisphere warm pool indices) and the onset date, demise date, seasonal length, and seasonal rain become more significant. However, these correlations are still weak when compared to the correlations of the onset and demise date to the seasonal length and seasonal rain. The variations in onset and demise dates of the rainy season over Central America influence the length and the seasonal rainfall variations of the rainy season significantly. Furthermore, the impact of onset and demise date variations on the corresponding seasonal length and seasonal rainfall is found to be relatively independent of each other. These correlations can be exploited for forecasting applications by utilizing real time monitoring of the rainfall to calculate the onset date. Further, there is considerable probabilistic skill shown with AROC maps. Values of AROC ≥ 0.5 for the outlook of an early/late onset with longer/shorter season length and wetter/dryer season (respectively) are widespread across Central America (Figure 22). With the availability of high-resolution rainfall data like IMERG, the proposed methodology can easily and effectively be adapted for real-time monitoring of the evolution of the wet season over this region.

This study offers a simple, but effective tool to provide an outlook of the forthcoming rainy season by simply monitoring the realization of the onset date of the wet season. The methodology, by way of generating an ensemble of estimates of onset and demise dates, allows for the generation of a probabilistic outlook of the wet season. Across most of Central America, an early or later onset date of the wet season is closely associated with the longer and wetter or shorter and drier seasonal length and rainfall anomaly of the wet season, respectively. The probabilistic skill scores of such an outlook also support the effectiveness of this local teleconnection. Therefore, the proposed monitoring of the local onset of the rainy season would be beneficial in the presence of stiff challenges in seasonal prediction by numerical climate models for the region.

4.3 Future Studies

The methodology used in this study has previously been successfully utilized for monitoring the monsoon season over India, Australia, and Florida as discussed in the introduction (Liebmann and Marengo 2001; Misra and DiNapoli 2014; Dunning et al. 2016; Uehling and Misra 2020). With the use of the IMERG dataset as in this study, the methodology can now be

implemented to any region on the globe at either a local or a regional scale which exhibits a strong seasonal cycle of rainfall. The code used in this study has been crafted to be shared and is being used in other regions including Southeast Asia and Africa.

Further studies into the Central America rainy season could include implementing the real-time monitoring application discussed in this paper. Real-time monitoring could be extremely useful to the economy of Central America, particularly the agricultural industry, which relies heavily on the rainy season. Another future study could be to look more broadly at the American monsoon system, which is likely related to the evolution of the Central American rainy season. It would be interesting to see the methods used in the study adopted on a much larger scale. As more time passes, revising this study with a larger time period of IMERG data could be insightful to larger scale patterns that are difficult to discern in this 22-years of data. Finally, adapting the methodology used in this study to be applied to the midsummer drought phenomenon and bimodal peak in the Central America rainy season could provide new insights into this impactful aspect of the rainy season.

REFERENCES

Alfaro, E. J., 2002: Some characteristics of the annual precipitation cycle in Central America and their relationship with its surrounding tropical oceans. Top. Meteorol. Oceanogr., 9, 88-103.

Alfaro, E. J., X. Chourio, A. G. Munoz, and S. J. Mason, 2017: Improved seasonal prediction skill of rainfall for the Primera season in Central America. Int. J. Climatol., https://doi.rog/10.1002/joc.5366.

Bhardwaj,A. and V. Misra, 2019: Monitoring the Indian Summer Monsoon Evolution at the Granularity of the Indian Meteorological Sub-divisions using Remotely sensed Rainfall Products Remote Sens. 11, 1080.

Huffman, G. J., Stocker, E. F., Bolvin, D. T., Nelkin, E. J., & Tan, J. (2019). GPM IMERG Final Precipitation L3 Half Hourly 0.1 degree x 0.1 degree V06, Greenbelt, MD, Goddard Earth Sciences Data and Information Services Center (GES DISC). https://doi.org/10.5067/GPM/IMERG/3B-HH/06

Dunning, C. M., E. C. L. Black, and R. P. Allan, 2016: The onset and cessation of seasonal rainfall over Africa. *J. Geophys. Res. Atmos.*, 121, 11,405– 11,424. doi:10.1002/2016JD025428.

Gramzow, R. H., and W. K. Henry, 1972: The Rainy Pentads of Central America. *J. Appl. Meteor. Climatol.*, **11**, 637–642, https://doi.org/10.1175/1520-0450(1972)011<0637:TRPOCA>2.0.CO;2.

Kowal, K. M., L. J. Slater, A. G. Lopez, and A. F. Van Loon, 2023: A comparison of seasonal rainfall forecasts over Central America using dynamic and hybrid approaches from Copernicus Climate Change Service seasonal forecasting system and the North American Multimodel Ensemble. Int. J. Climatol., https://doi.org/10.1002/joc7969.

Liu, C. and E. Zipser, 2013: Regional variation of morphology of organized convection in the tropics and subtropics. J. Geophys. Res. Atmos., 118, 453-466.

Magana, V. O., J. A. Amador, S. Medina, 1999: The mid-summer drought over Mexico and Central America. J. Clim., 12, 1577-1588.

Misra, V., H. Li, and M. Kozar, 2014: The precursors in the Intra-Americas Seas to seaseasonal climate variations over North America J. Geophys. Res. (Oceans), 119(5), 2938-2948, doi:10.1002/2014JC009911.

Misra, V., and S. DiNapoli, 2014: The variability of the Southeast Asian summer monsoon. Int. J. Climatol., 34(3), 893-901, https://doi.org/10.1002/joc.3735.

Misra, V., D. Groenen, A. Bharadwaj, and A. Mishra, 2016: The warm pool variability of the tropical northeast Pacific Int. J. Climatol., doi:10.1002/joc.4658.

Misra, V., C. B. Jayasankar, P. Beasley, and A. Bhardwaj, 2022: Operational Monitoring of the Evolution of the Rainy Season over Florida Front. Clim., 4, 793959, doi:10.3389/fclim.2022.793959.

Misra, V., S. Dixit, and C. B. Jayasankar, 2023: The Regional Diagnosis of Onset and Demise of the Rainy Season over Tropical and Subtropical Australia Earth Interactions, https://doi.org/10.1175/EI-D-22-0026.1.

Nakaegawa, T., O. Arakawa, and K. Kamiguchi, 2015: Investigation of Climatological Onset and Withdrawal of the Rainy Season in Panama Based on a Daily Gridded Precipitation Dataset with a High Horizontal Resolution. *J. Climate*, **28**, 2745–2763, https://doi.org/10.1175/JCLI-D-14-00243.1.

Narotsky, C. D. and V. Misra 2022: The Seasonal Predictability of the Wet Season over Peninsular Florida Int. J. Climatol., https://doi.org/10.1002/joc.7423.

Reynolds, R.W., N.A. Rayner, T.M. Smith, D.C. Stokes, and W. Wang, 2002: An improved in situ and satellite SST analysis for climate. J. Climate, 15, 1609-1625.

Taylor, M.A., Alfaro, E.J. (2005). Central America and the Caribbean, Climate of. In: Oliver, J.E. (eds) Encyclopedia of World Climatology. Encyclopedia of Earth Sciences Series. Springer, Dordrecht . https://doi.org/10.1007/1-4020-3266-8_37.

Uehling, J. and V. Misra, 2020: Characterizing the seasonal cycle of the Northern Australian rainy season. J. Climate, 33, 8957-8973.

Vera, C., W. Higgins, J. Amador, T. Ambrizzi, R. Garreaud, D. Gochis, D. Gutzler, and coauthors, 2006: Toward a unified view of the American monsoon systems. J. Climate, 4977-5000, https://doi.org/10.1175/JCLI3896.1.

BIOGRAPHICAL SKETCH

Joanna Marie Rodgers was born and raised near Newnan Georgia where she attended the University of West Georgia. At the University of West Georgia, she was a teaching assistant for both Chemistry and Weather and Climate labs. She also was a funded researcher, working with Dr. Shea Rose using ArcGIS Pro to study the spatial and temporal trends of tornadoes in the United States. After graduating from the University of West Georgia in May 2021 with a Bachelor of Science in physical geography, she attended Florida State University to receive a Master of Science in meteorology. During her time at Florida State University, she worked as a teacher assistant and would lead beginner meteorology labs. The results presented in her master's thesis have been submitted to Geophysical Research Letters in hopes of a publication.